



Photocatalytic sponges for wastewater treatment, carbon dioxide reduction, and hydrogen production: a review

Akash Balakrishnan¹ · Meenu Mariam Jacob² · Mahendra Chinthala¹ · Nanditha Dayanandan² · Muthamilselvi Ponnuswamy² · Dai-Viet N. Vo³

Received: 11 October 2023 / Accepted: 9 January 2024 / Published online: 16 February 2024
© The Author(s), under exclusive licence to Springer Nature Switzerland AG 2024

Abstract

Water pollution and the energy demand are calling for sustainable technologies such as photocatalysis, yet actual methods are difficult to upscale due to the poor recovery and reusability of nanocatalysts. This issue could be solved by using photocatalytic sponges, which display high surface area and reusability. Here we review the applications of photocatalytic sponges for wastewater degradation, disinfection, carbon dioxide reduction, and hydrogen production. Photocatalytic sponges are fabricated by templating, dip coating, sol–gel, polymerization, electrospinning, and freeze drying. Remarkable results include the monolithic microreactor with Ag/AgCl coated on a polydopamine-modified melamine sponge, which exhibits a 100% methylene blue degradation in 15 min, with a reusability of five cycles. An hydrogen production rate of 11.33 mmol h⁻¹ g⁻¹ was obtained with the pyridazine-doped graphitic carbon nitride with nitrogen defects and a spongy structure.

Keywords Carbon dioxide reduction · Energy · Organic pollutants · Photocatalyst · Wastewater

Introduction

In the current scenario, the world is facing several critical challenges due to the ever-increasing energy crisis and global environmental pollution (Liang et al. 2021b). As per the report of the United Nations International Children's Emergency Fund, in developing countries, about 1.2 billion people do not have access to clean and safe drinking water (Usman et al. 2022). Innumerable reports have been made about the persistence and alleviation of organic pollutants

including pharmaceuticals, pesticides, drugs, dyes, poly-fluorinated compounds, heavy metals, and micro-plastics in different water bodies, including drinking water (Tijani et al. 2016; Picó et al. 2020; Balakrishnan et al. 2022b). The abundant presence of these organic pollutants is causing a major threat to the environment and humans (Scaria et al. 2021). On the other hand, the continuous carbon dioxide emissions and excessive combustion of fossil fuels induce global warming (Anderson et al. 2016).

Among all the conventional water treatment technologies, photocatalysis has recently emerged as a versatile, environmentally benign approach for the management of energy and environmental issues (Sarkar et al. 2020; He et al. 2021; Balakrishnan et al. 2023a). The potential applications of these technologies include wastewater treatment, disinfection, hydrogen generation, and carbon dioxide conversion to fuels or fine chemicals (Balakrishnan and Chinthala 2023; Wen et al. 2017). Over the years, plenty of photocatalysts have been developed based on titanium dioxide (TiO₂), graphitic carbon nitride (g-C₃N₄), zinc oxide (ZnO), cadmium sulfide (CdS), and zinc sulfide (ZnS) that are employed in energy sectors as well as environmental remediation (Jbeli et al. 2018; Zhang et al. 2020; Liu et al. 2023b; Kong et al. 2022; Balakrishnan and Chinthala 2023). Among these

✉ Mahendra Chinthala
chinthalam@nitrrkl.ac.in

✉ Dai-Viet N. Vo
vndviet@ntt.edu.vn

¹ Process Intensification Laboratory, Department of Chemical Engineering, National Institute of Technology Rourkela, Rourkela, Odisha 769 008, India

² Department of Chemical Engineering, College of Engineering and Technology, SRM Institute of Science and Technology, Chengalpattu, Tamil Nadu 603 203, India

³ Center of Excellence for Green Energy and Environmental Nanomaterials, Nguyen Tat Thanh University, Ho Chi Minh City, Vietnam

catalysts, titanium dioxide (TiO_2) and graphitic carbon nitride ($\text{g-C}_3\text{N}_4$), along with other graphene-based carbon materials, have been prominently employed due to the higher photocatalytic activity in ultraviolet and visible regions (Balakrishnan and Chinthala 2022). The difficulties of recovery and reuse decreased photocatalytic stability, decreased adsorption of pollutants, and high cost of the nanopowder photocatalyst make them unsuitable for large-scale applications (Balakrishnan et al. 2022b, a). An effective strategy to overcome these problems is the development of three-dimensional sponges for photocatalysis (Chen et al. 2022). The sponges are porous materials that are composed of a catalytic component with a sponge structure (Hossain et al. 2020). The combination of foam and photocatalyst can be beneficial to overcome the common drawbacks of photocatalysts, including recovery, reusability, higher surface area, and porosity (Sun et al. 2022) (see Fig. 1). The unique properties make the photocatalytic sponges ideal for the remediation of dyes, pharmaceuticals, phenolics, and pesticides. However, no comprehensive review has yet elaborated on the preparation, properties, and applications of photocatalytic sponges.

This review discusses the preparation, properties, and applications of photocatalytic sponges along with potent applications in areas of photocatalytic degradation of organic pollutants, including dyes, pesticides, pharmaceuticals, and phenolic compounds, disinfection, hydrogen evolution, and carbon dioxide conversion into

fine chemicals. Firstly, the general characteristics and commonly employed supports of photocatalytic sponges are explained in detail. The succeeding section highlights the fabrication methods and properties of photocatalytic sponges. Finally, a comprehensive review is conducted on the versatile applications of sponges in energy and environmental applications. The advantages, disadvantages, and perspectives of the photocatalytic sponges are critically discussed in relation to the existing photocatalytic materials.

Photocatalytic sponges

Sponges are highly porous three-dimensional structures inspired by the aquatic animals of the *Phylum Porifera*, which is composed of porous surfaces (Zhu et al. 2017). These usually consist of fibrous materials arranged in complex porous structures in regular or irregular patterns (Zhao et al. 2022). The dense three-dimensional structure of sponges exhibits distinctive characteristics such as extraordinary surface area, porosity, simplicity in preparation, compressibility, good mechanical strength, low density, pore volume, and diverse preparation methods (Hossain et al. 2020; Wang et al. 2020b; Xu et al. 2021). Melamine and polydimethylsiloxane sponges have been employed along with biopolymeric sponges in diverse applications, including catalysis, water treatment, energy conversion, drug delivery, and tissue engineering (Zhu

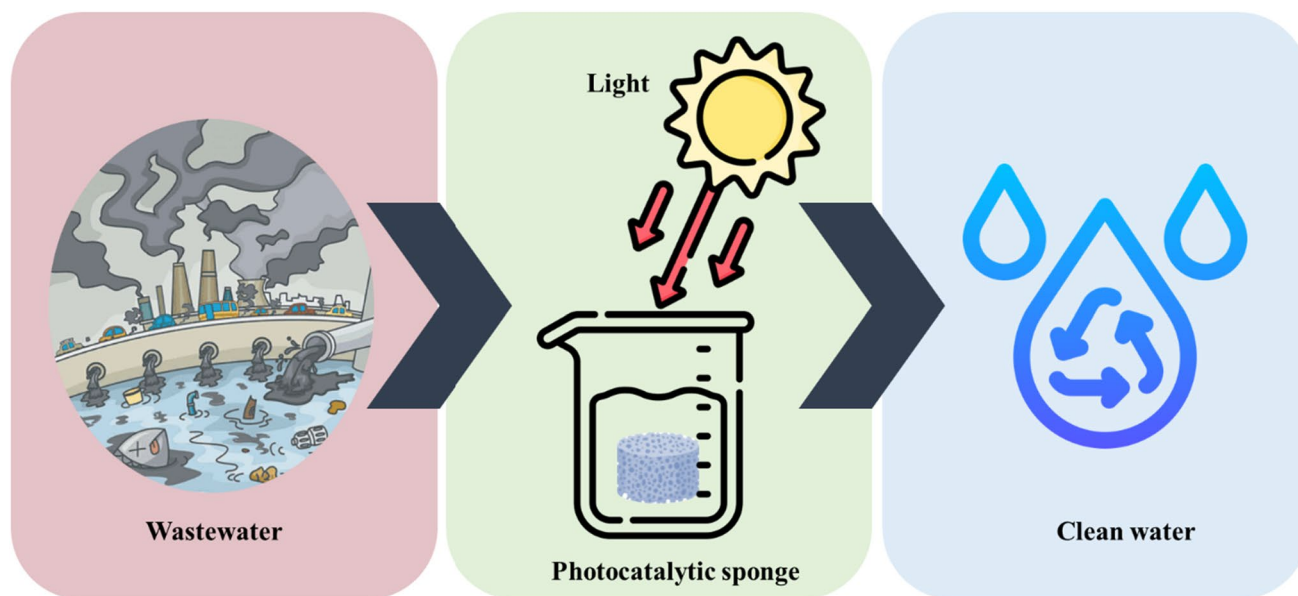


Fig. 1 Photocatalytic treatment of wastewater using sponge. Photocatalytic sponges offer a versatile and efficient solution for water treatment because they can use light to activate materials that are incorporated with photocatalysis. These sponges contribute to a thorough and long-lasting approach to environmental restoration by

efficiently targeting and degrading a variety of pollutants, including organic contaminants and even some pathogens. Furthermore, the sponges' porous structure increases their capacity for adsorption, which enables them to collect and eliminate contaminants from water sources effectively.

et al. 2017; Lei et al. 2017; Sukul et al. 2021). The sponges are affordable, flexible, elastic, and have a facile design (Peçenek et al. 2022), which makes them easily adoptable as suitable supports for photocatalysts due to the non-toxicity and extremely safe, higher chemical stability, good photostability, flexibility, and lower weight, durability (Tu et al. 2019; Sosnin et al. 2021). Therefore, minuscule molecule mass transfer and diffusion have a special focus on the three-dimensional matrices.

Photocatalysis is a versatile treatment technology adopted for diverse applications. The efficacy of a photocatalytic process relies on the type of catalytic material, process parameter, light irradiation, and reactor design (Mudhoo et al. 2020; Balakrishnan et al. 2022b). As a result, the actual uses of these materials in industries are not well-established. Traditional photocatalysts, including titanium dioxide (TiO₂), zinc oxide (ZnO), and zinc sulfide (ZnS), were initially employed as nanoparticles. Despite the photocatalytic efficiency, environmental concerns grow as a result of nanoparticles seeping into aquatic matrices. These nanopowder catalysts were not economically feasible due to difficult recovery operations and poor reusability (Balakrishnan et al. 2023b, c, a). The notion of immobilized photocatalysts overcame these traditional limits of poor reusability and recoverability but possessed very low surface area and exhibited poor mass transfer. To address all these challenges, the concept of photocatalytic sponges was proposed. The high porosity and surface area

on the structure of sponges ensure effective interaction between light source and catalytic particles.

The photocatalytic sponges demonstrate higher potential in terms of efficacy, stability, reusability, and suitability for large-scale applications. Greater adsorption rate and exceptional mechanical stability are further benefits. These materials have different levels of macro- and micro-porosity. The photocatalytic sponges' larger surface areas provided a lot more active sites, which speed up the generation of reactive oxygen species and photocatalysis. Various methods can be used to develop the sponges into a wide range of shapes and forms. Researchers have already proved that the sponges are predominant over nanoparticles; however, in major cases, the nanocatalysts are coated onto commercially available sponges such as polydimethylsiloxane, polyurethane, polyvinyl alcohol, and melamine sponges (Sam et al. 2021). The characteristics of different commercially available sponges are discussed in Table 1. Alginate, cellulose, and chitosan-based sponges have also been produced in recent years due to high availability, abundance, and safety (Balakrishnan et al. 2022a).

Fabrication routes

To alter the hydrophilic surface to a hydrophobic surface, it is imperative to establish practical, simple, and effective methods. The commonly employed strategies are dip coating, the in situ method, freeze drying, carbonization,

Table 1 Most of the commercially available sponges as photocatalytic supports include polymers with exceptional properties. All the sponges are porous with high surface area and good elasticity

Sponge	Description	Properties	References
Polyurethane	Polyurethane is composed of organic units connected via urethane links	<ul style="list-style-type: none"> • Higher porosity and surface area • Good elasticity • Easy to recover and reuse • Good adsorption ability 	Sam et al. (2021)
Melamine	Melamine sponges resemble a dense solid and are an air-filled lattice framework of the material called formaldehyde-melamine-sodium bi-sulfite copolymer	<ul style="list-style-type: none"> • Lower cost • High flexibility and density • Easy to surface modification • Resistant to high temperature • Non-toxic to environment 	Liang et al. (2015), Sam et al. (2021)
Polyvinyl alcohol	Polyvinyl alcohol sponge is a synthetic sponge composed of a vinyl polymer connected via carbon-carbon linkages	<ul style="list-style-type: none"> • Expandable • High tensile strength • Resistant to chemicals • Highly porous 	Gao et al. (2022c)
Polydimethylsiloxane	Polydimethylsiloxane is composed of methylated siloxane polymers with repeating units and trimethylsiloxy end-blocking units	<ul style="list-style-type: none"> • Chemically inert • Good thermal stability • Easy to tune the properties • High porosity • High reusability 	Sosnin et al. (2021)
Biopolymers	The biopolymers including cellulose, chitosan, and sodium alginate, are employed	<ul style="list-style-type: none"> • Non-toxic and safe • Higher reusability • Lower cost and ease of availability 	Balakrishnan et al. (2022a)

chemical vapor deposition, polymerization, and thermal methods, which are elucidated in detail.

Templating methods

The templating methods are the commonly adopted sponge preparation strategy with the help of a suitable solid or emulsion. Templating methods are broadly divided into direct templates and emulsion templates. The direct template approach, which uses solid templates as porogen and can be entirely removed to produce sponges with well-connected cavities, is the simplest way to create sponges. Direct template methods can be split into two categories depending on the application of a template. Sacrificial templates made of polymer particles, nickel foam, salt crystals, and sugar cubes can be used as templates (Zhu et al. 2017). It is more practical to use the leaching of salt or sugar cubes due to (i) no requirement of sophisticated types of equipment and (ii) minimum usage of solvents.

Sugar cubes can be selected as the sacrificial template that can be placed in an appropriate reactor for the molding of a suitable elastomer (Lee et al. 2019). Followed by the addition of a mixture of pre-polymer and curing agents (dimethicone) into the bath to submerge the sugar cubes, the yielded solution can be degassed in a vacuum chamber to help infiltration of the liquid pre-polymer to sugar cube voids, which is to be kept in an oven. The cubes of cured polymer sugar are chopped into pieces to expose the sugar template, and then the sugar is leached out to create a three-dimensional porous sponge (Lee et al. 2020). The particle size and mixing ratio with the prepolymer solution in the particle leaching process make it simple to modify the sponges' pore size and porosity. A higher concentration of particles in the prepolymer solution during the mixing of both substances would lead to the formation of interconnected pores (Zhu et al. 2017).

The gold (Au) nanoparticles supported the floating porous polydimethylsiloxane sponge, which was developed using the simple sugar template method and has demonstrated significant stability (Lee et al. 2020). The direct templating method is also used for the fabrication of sponges with micron-sized pores. The key advantages of the templating technique are tunable pore size and porosity, high affordability, reliability, and well-arranged pore structures with well-attached pore interconnection. However, the utilization of hazardous solvents is the main drawback of a templating method for the preparation of sponges using sacrificial templates, including inorganic and polymeric materials.

In the emulsion template method, sponges are prepared through the polymerization of an emulsion, where emulsion droplets resemble a template for the formation of pores (Timusk et al. 2022). Controlling the stability

of the liquid emulsion template for the process of aging equivalent to the coalescence of droplets is always desirable for the achievement of the required pore structure. The interconnected and separated pores can both develop via the templating method possessing narrow size distribution (Zhu et al. 2017). The major advantages of emulsion templating are highly tunable porosity, pore size, and the ability to develop open and closed pore structures. The persistence of surfactant inside the polymer may affect the properties of the sponges during the preparation stage. The elimination of the surfactant is often considered a difficult task and requires more time. Researchers adopted the emulsion templating method for the development of sponges for environmental remediation.

Dip coating

Dip coating is the common and simplest preparation strategy adopted to yield sponges, as highlighted in Fig. 2a. Here, sponges are immersed in a solution composed of modified materials and lifted vertically from the solution (Elshof et al. 2015). The photocatalytic sponges are then obtained by drying the immersed sponges. For example, Fang et al. (2018) fabricated molybdenum sulfide (MoS_2) nanoflowers through the hydrothermal method and grafted them on melamine formaldehyde sponge through a dip-coating strategy to yield molybdenum sulfide (MoS_2) nanoflower sponges. Here, the melamine sponge was cleaned with acetone, ethanol, and water and dried before dipping into a molybdenum sulfide (MoS_2) solution. It was dried at 60 °C for two hours. The process of dipping and drying was continued three times to attain uniformity on the photocatalytic sponges. The merits of dip coating are lower cost, and the thickness can be altered. However, the process is relatively slower and possesses the ability to block the screen, which poses an adverse effect on the final sponge (Kakaei et al. 2019).

Sol-gel

The sol-gel process is one of the most used strategies adopted for the preparation of sponges (Peng et al. 2015). The sol-gel process involves three major steps, namely: sol-gel process, aging, and drying. Initially, the hydrolysis and partial condensation of the alkoxide yields a sol commonly known as a colloidal suspension. In the presence of a catalyst, the gel is created through polycondensation (Reddy et al. 2020). Fine solid particles scattered in the gel during gel formation take on a three-dimensional structure. The rate of condensation and hydrolysis affects the gel's structure, while the ratio of water to alkoxide and the choice of solvent affects the other variables. In the second step, sufficient time is provided to ensure complete polycondensation and re-precipitation

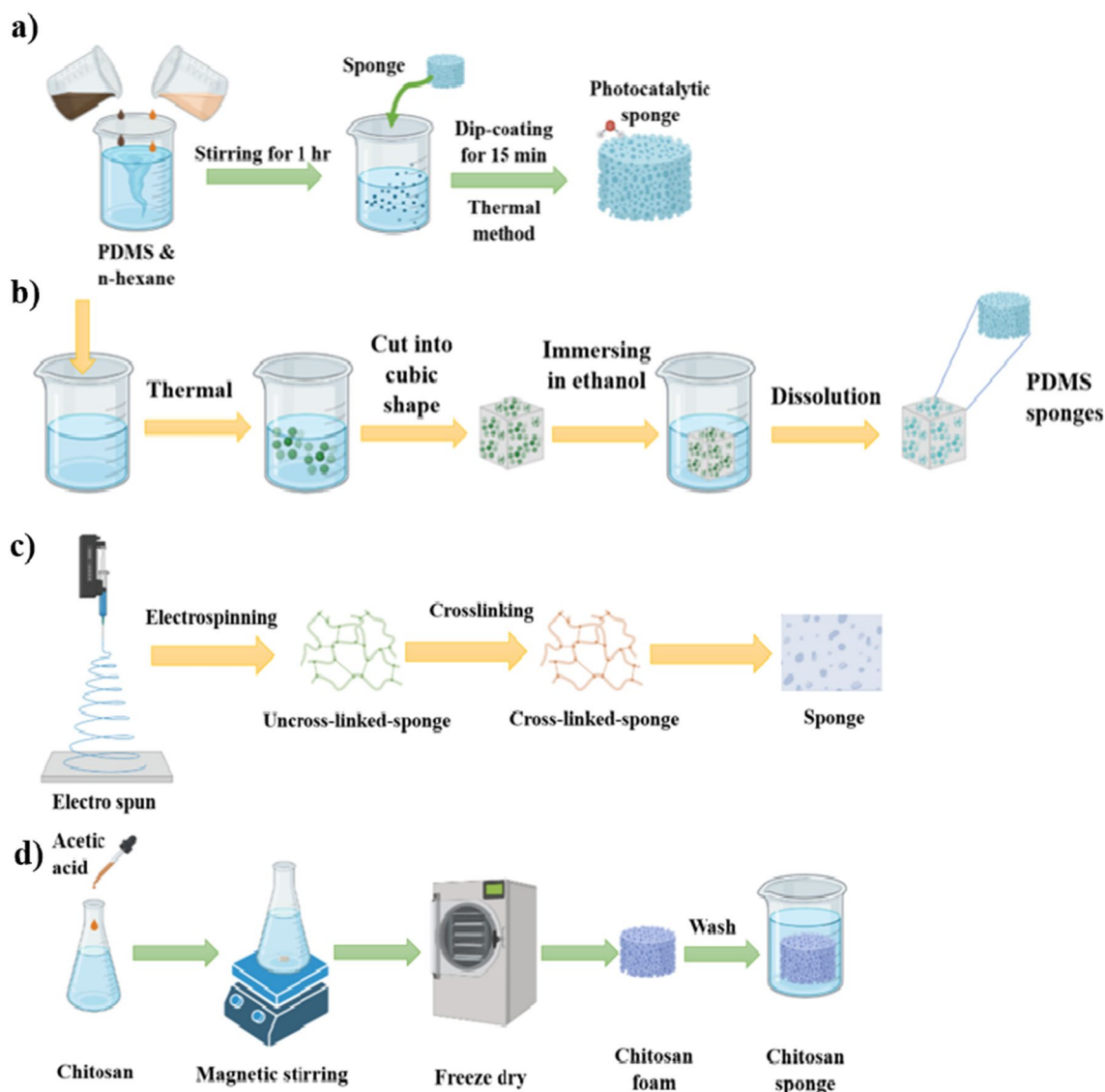


Fig. 2 The commonly employed preparation routes of photocatalytic sponges: **a** Dip coating is a simple procedure in which the sponges are dipped into photocatalytic nanoparticle solution multiple times and dried; **b** polymerization involves the cross-linking of nanoparticles with the polymer to form the polymer chains; **c** electrospinning is

the efficient strategy to produce the ultrafine fibers through charging and ejecting a polymer melt under high voltage, and **d** freeze drying is a process in which water is easily sublimated via the direct transition of water from solid to vapor. PDMS stands for polydimethylsiloxane

of the interconnected network gels (Jiang et al. 2017). The gels are finally dried to create a three-dimensional structure, where the gel's solvents have been replaced with air (Sirajudheen et al. 2021; Jiang et al. 2017). The merits of sol–gel methods include (i) easy fabrication, (ii) production of high-quality material with uniformity and higher purity, and (iii) higher surface area (Kumar et al. 2020). The higher time requirements and the consumption of organic solvents during the preparation of sponges are undesirable characteristics of the sol–gel method (Jiang et al. 2017).

Polymerization

A polymer is cross-linked in the polymerization process to create polymer chains (Paszkievicz et al. 2019). As shown in Fig. 2b, the polymer also acts as a cross-linking agent, joining materials with sponge surfaces to create hydrophobic sponges. Most commonly, dopamine is selected as a cross-linking agent due to its self-polymerization capability and stability with covalent and non-covalent bonding forces (Peng et al. 2019). For instance, Gao et al. (2022a, b, c) prepared a carbon nitride/polyvinyl alcohol sponge by dissolving polyvinyl alcohol in water, followed by keeping

it in an oil bath at 95 °C. Followed by the addition of formaldehyde solution and 2-(2-[4-(1,1,3,3-tetramethylbutyl)phenoxy]ethoxy) ethanol into hot polyvinyl alcohol solution yields a foam. The foam solution was then dried to produce the sponges, and then sonicated carbon nitride-treated sulfuric acid was added (Gao et al. 2022c). The use of surfactants or stabilizers is not needed for the polymerization process in order to tune the shape or size of the catalyst. However, higher time requirements and larger solvent consumption are the major drawbacks of polymerization (Sirajudheen et al. 2021).

Electrospinning

Electrospinning is a prominent technique for the generation of various micro- or nanofibrous structures with diverse uses in the domain of catalysis, drug delivery, and water treatment (Wang et al. 2020a). The threads are produced from the polymer solution using electric forces in the electrospinning procedure shown in Fig. 2c (Bazrafshan et al. 2019; Balakrishnan et al. 2022a). For instance, Mi et al. (2018) reported the self-assembly electrospinning route for the preparation of silica sponges. Initially, a thin layer of flat fibers was produced and slowly grown. Further, the height of the stack reached ten cm after spinning, followed by calcination at 800 °C. The produced silica sponges were light in weight and easily formed into any desired shapes by compressing or twisting (Mi et al. 2018). The electrospinning method produces a high surface area hierarchical nano- or micro-three-dimensional porous structure. The main drawback is the consumption of solvents, which may affect the porous structure of the sponges (Sirajudheen et al. 2021).

Freeze drying

Freeze drying is removing the solvent by sublimation of frozen solution under a high vacuum environment (Rostamabadi et al. 2021). Freeze drying involves two major steps, namely, thermally stimulated phase separation followed by solvent sublimation at very low pressure, as seen in Figs. 2d. The phase separation yields lean polymer and polymer-rich phases that are formed at a definite temperature in an unstable polymer solution. The freeze drying causes the sublimation of solvent to yield a sponge. For instance, Chen et al. (2022) described the fabrication of cellulose nanofibril/rectorite composite sponge through directional freeze drying of cellulose nanofibril/rectorite dispersion. The advantages of freeze drying are the low-temperature process, easily molded into the desired shape without being interfered with by the elimination of solvent molecules, and the hierarchical porous structure is crucial in ensuring efficient mass transfer (Ma et al. 2019). Freeze drying is a simple, easy, versatile, and scalable method but is a little expensive compared to spray drying (Rostamabadi et al. 2021). Table 2 summarizes the advantages and disadvantages of different fabrication methods.

Properties of sponges

Photocatalytic sponges are widely studied porous crystalline materials due to their unique hitherto properties. A variety of photocatalytic sponges are developed using polymeric and biopolymeric materials, and the applications of sponges are based on the structural, morphological properties, surface area, stability, durability, and crystallinity.

Table 2 Fabrication routes of photocatalytic sponges with their advantages and disadvantages

Preparation route	Advantage	Disadvantage	References
Direct templating	<ul style="list-style-type: none"> Well-interconnected pore structure Facile and affordable preparation route Easy to alter pore size and porosity 	The requirement for hazardous solvents	Zhu et al. (2017)
Emulsion templating	<ul style="list-style-type: none"> Pore size is down to microns Easy to tune porosity Able to yield both open and closed pore structure Monodisperse pore size can be achieved 	The secondary pollution caused by surfactants and organic solvents	Zhang et al. (2019b)
Dip-coating	<ul style="list-style-type: none"> Low-cost preparation method Easy to tune the thickness 	High time requirements	Sahoo et al. (2018)
Sol-gel	<ul style="list-style-type: none"> Good purity Low processing temperature Good adhesion Ability to coat the complex substrate 	<ul style="list-style-type: none"> Longer time requirements Not able to attach a dense layer of catalyst particles on the substrate Higher cost for fabrication 	Balakrishnan et al. (2022b, a)
Electrospinning	Able to control the size of the fibers	<ul style="list-style-type: none"> Requires the use of toxic solvent Not applicable for larger scaffolds 	Sirajudheen et al. (2021)

Photocatalytic sponges possess a three-dimensional structure with highly interconnected pores and predominantly larger pore volume. The porosity and surface area are the desirable advantages of the photocatalytic sponges, making the sponges ideal for different applications in environmental remediation. The porous structure always acts as a platform for effective interaction between the host and guest chemistry on the interior or exterior of the host. The cellulose chitosan sponge exhibited a high surface area of $178.9 \text{ m}^2 \text{ g}^{-1}$, which is ascribed to the formation of thick walls inside the sponge (Zhang et al. 2019a).

Islam et al. (2019) reported that cobalt sponge ($17.3 \text{ m}^2 \text{ g}^{-1}$) exhibited a higher surface area than nickel sponge ($8.8 \text{ m}^2 \text{ g}^{-1}$) and copper sponge ($2.7 \text{ m}^2 \text{ g}^{-1}$). Figures 3a shows the morphology of zinc sulfide (ZnS)/cellulose chitosan sponges exhibited a cylindrical shape with an intact structure. The cross-sectional view affirms the presence of macropores (see Fig. 3b and c) with a size of $200 \mu\text{m}$ and a porosity of 83% (You et al. 2022). Figure 3d and e shows the honeycomb structure with a dense porous

structure of cellulose nanofibril/rectorite composite sponge in the transverse direction. The presence of pore channels identified in Figs. 3h in the longitudinal direction affirms structural anisotropy. The characteristic peaks of silicon (Si) and aluminum (Al) are shown in Fig. 3f and g. The uniform distribution of these elements on the pore walls is shown in Fig. 3i and j, which show the agglomeration at 1:1 ratio of nanofiber and rectorite (Chen et al. 2022). The sponges can be formed into any desired shapes and found to be light weight. The three-dimensional hierarchical highly porous structure supplies an abundant number of catalytic active sites toward the photocatalytic reaction, improves the separation efficiency, and reduces the diffusion path of electron–hole species (Yao et al. 2022).

The photocatalytic sponges also demonstrate the chemical and thermal stability. The three-dimensional macro-/mesoporous titanium dioxide (TiO_2) sponge prepared through the gelation of lotus root starch capable to withstand up to $550 \text{ }^\circ\text{C}$ is ascribed to the inclusion of the titanium dioxide (Wang et al. 2014). The graphitic carbon nitride

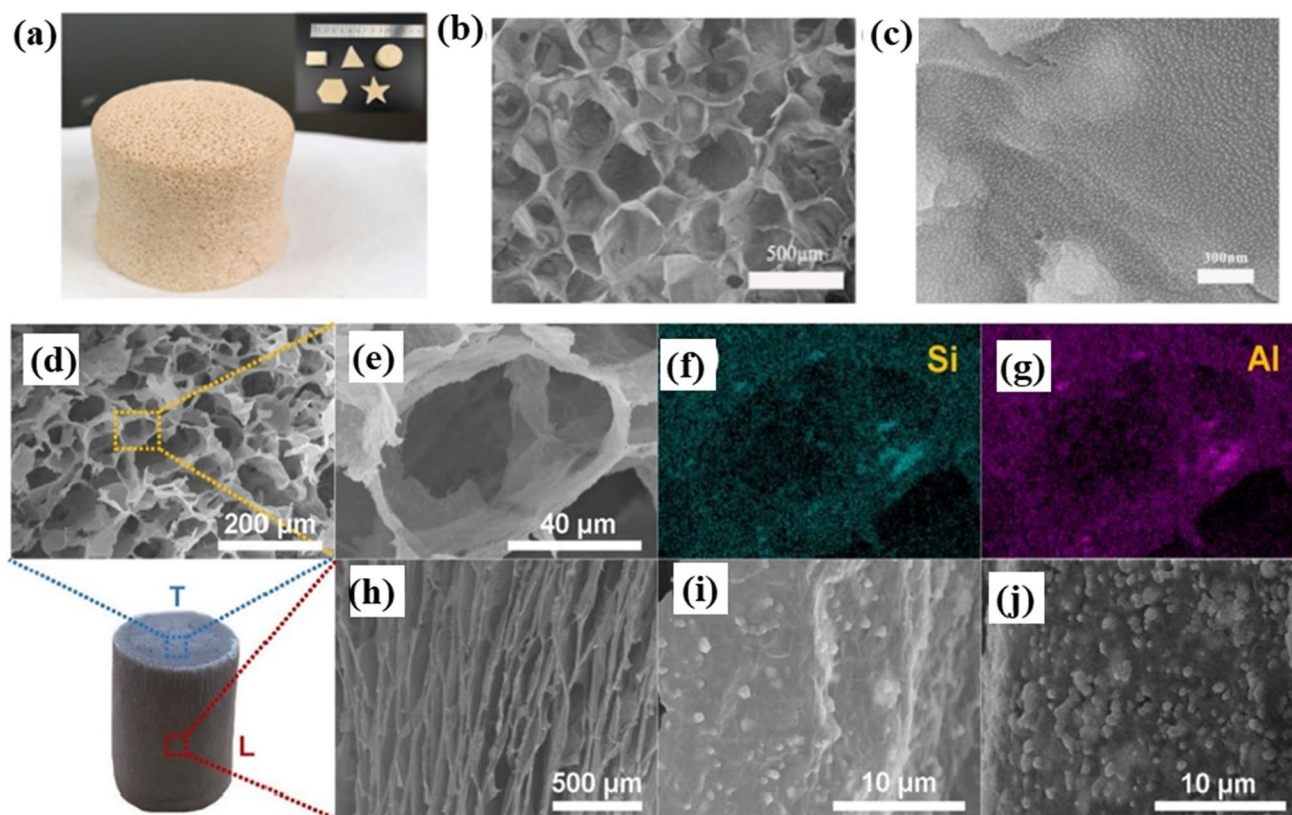


Fig. 3 a Photograph of zinc sulfide (ZnS)/cellulose chitosan sponge indicated a three-dimensional porous structure. Scanning electron microscopy image of **b** sponge skeleton and **c** zinc sulfide (ZnS)/sponge. Reprinted with permission of Elsevier from reference (You et al. 2022). Scanning electron microscopy images of the sponges' cellulose nanofibril/rectorite composite sponge, **d** top view, **e** cor-

responding higher magnification, **f-g** elemental mapping, **h** inside view, **i** corresponding higher magnification, and **j** scanning electron microscopy image cellulose nanofibril/rectorite composite sponge. Reprinted with permission of Elsevier from reference (Chen et al. 2022). Si is silicon, and Al is aluminum

(g-C₃N₄)-polydimethylsiloxane sponge displayed good thermal stability by retaining 82% of the initial weight at 550 °C. The sponge was able to survive the extremely harsh corrosive environment for over forty-five hours compared to the bare polydimethylsiloxane sponge (Abdelhafeez et al. 2020). The enhanced thermal stability and chemical stability are ascribed to the inclusion of effective catalytic materials into the sponge.

The photocatalytic sponges displayed outstanding mechanical properties, eventually increasing their usage. The pristine sponge exhibits greater flexibility, elasticity, and durability, making it an ideal template for the preparation of sponges. For instance, in graphitic carbon nitride (g-C₃N₄)/polyvinyl alcohol composite sponge, the tensile strain increases with an increase in the tensile stress. At 300% strain, the graphitic carbon nitride(g-C₃N₄)/polyvinyl alcohol composite sponge is about to break. The prepared graphitic carbon nitride (g-C₃N₄)/polyvinyl alcohol sponge possessed high elastic deformation ability. The composite sponges were easily bent, compressed, and easily returned to the actual structure without affecting the structure of the sponge (Gao et al. 2022c). The zinc sulfide (ZnS)-supported cellulose/chitosan sponge exhibited very high structural stability through the fatigue hysteresis test of the compression cycle. The zinc sulfide (ZnS)-cellulose/chitosan sponge could easily be recovered after being compressed by 80%, and the maximum stress of the sponge was reduced by 10% after twenty compression cycles (You et al. 2022).

Similarly, a three-dimensional lignosulfonate composited sponge impregnated with bismuth vanadate/polyaniline/silver ternary photocatalytic sponge can be compressed into thin sheets and recovered back to normal shape after soaking with water. The compressive strength of the sponge is increased from 0.052 to 0.105 MPa after the incorporation of a photocatalyst into the sponge (Gao et al. 2022b). Similarly, the compressive strength of the three-dimensional sponge complexed molybdenum sulfide (MoS₂)/bismuth sulfide (Bi₂S₃)/bismuth vanadate (BiVO₄) is increased from 0.049 to 0.148 MPa after the incorporation of ternary photocatalysts into the sponge (Gao et al. 2022a). Almost all the researchers reported an increment in mechanical properties and retained it back to its normal structure. The phenomenal mechanical properties are responsible for the reusability of sponges.

The photocatalytic sponges are highly reusable for several cycles due to their outstanding deforming capability, which makes them suitable for practical applications. After the photocatalytic study, the sponges are recovered and washed with water multiple times, squeezed, and dried before the next degradation study. For example, Hossain et al. (2020) reported the reusability of ten cycles against Methylene Blue. The polydopamine-functionalized sponge also exhibited a reusability of ten cycles toward the degradation of Methylene Blue by using an ethanol–water

mixture for cleaning the sponge fiber each cycle in the ratio of 1:1 (Zhang et al. 2019c). These results proved that the photocatalytic sponges are highly reusable and easily recovered without any losses in the catalyst. The versatile properties of the hybrid sponges make them suitable for environmental remediation.

Applications

The inherent qualities of photocatalytic sponges led to a variety of applications. We discuss the applications of photocatalytic sponges in the areas of environmental remediation, and energy conversion is elucidated. The catalytic activity of the sponges is ascribed to the porous structure with high surface area, chemical and thermal stability, affordability and environmental friendliness. Figure 4 showcases different applications of photocatalytic sponges in water treatment, disinfection, hydrogen evolution and carbon dioxide reduction.

Photocatalytic degradation of organic pollutants

The increased contamination of aquatic systems with pharmaceuticals, pesticides, dyes, and phenols alarms the livelihood of our ecosystem (Shi et al. 2020; Balakrishnan et al. 2023b). Researchers were drawn to photocatalytic

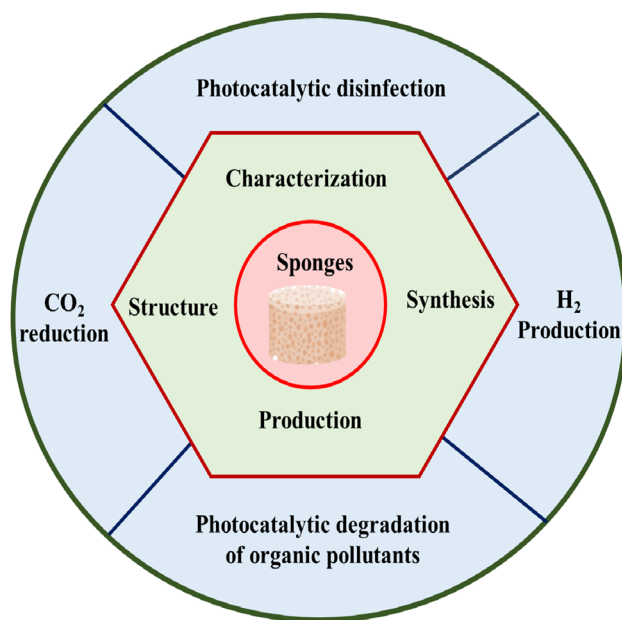


Fig. 4 Applications of photocatalytic sponges in energy and environmental remediation. The potent applications of photocatalytic sponges include wastewater remediation, disinfection, hydrogen production, and carbon dioxide sequestration. Among them, the majority of the studies are explored toward the photocatalytic degradation of dyes

water treatment technology over adsorption because this technology is more environmentally friendly (Rajagopal et al. 2020; Chinthala et al. 2021). The fundamental mechanism is to oxidize the sponge photocatalyst to degrade the organic pollutants with the assistance of ultraviolet or visible light. The sponge-based photocatalysts exhibit great catalytic activity due to their highly porous three-dimensional structure, abundant active sites, and enhanced adsorption.

The majority of researchers have conducted the removal of dyes rather than other organic contaminants due to the higher accessibility and ease of analysis. For instance, Gao et al. (2022c) developed stable and highly elastic graphitic carbon nitride ($g\text{-C}_3\text{N}_4$)/polyvinyl alcohol sponges via the co-polymerization method. The prepared sponge composites exhibited predominant porosity, and elastic deformation property makes them adaptable to attain different shapes. The photocatalytic degradation studies reported a 79% elimination of tetracycline within 80 min. The total organic carbon removal studies stated a maximum removal of 58% and 76% for Rhodamine B and tetracycline, respectively. The sponges exhibited a recyclability of ten cycles toward the Rhodamine B. The elastic graphitic carbon nitride/polyvinyl alcohol sponges can be easily tailored to a larger scale due to durability and outstanding stability. The predominant catalyst efficiency is ascribed to improved optical properties and porosity.

You et al. (2022) developed zinc sulfide (ZnS)-supported cellulose/chitosan sponges through an in situ method for the removal of Congo Red. Here, zinc sulfide-supported cellulose/chitosan sponges were developed through the hydrothermal decomposition of xanthates and the in situ preparation of zinc sulfide. The structural studies proved the porous (83% porosity) skeleton structure composed of different flexible transport routes with phenomenal mechanical strength. The photocatalytic studies demonstrate a maximum efficiency of 96% under the illumination of ultraviolet irradiation. The superoxide and hydroxyl radicals played a vital role in the destruction of organic dyes. The sponges also demonstrated a maximum reusability of eight cycles with an efficiency of 85%.

Hickman et al. (2018) emphasized that titanium dioxide (TiO_2)-polydimethylsiloxane hybrid sponges, a hydrophobic sponge for the destruction of Rhodamine B, were fabricated by using sugar as a template. Scanning electron microscopy images proved the three-dimensional framework of polydimethylsiloxane with a successful amalgamation of titanium dioxide (TiO_2) with greater porosity. The solar-light-assisted photocatalytic degradation was able to remove Rhodamine B effectively due to the synergistic action of titanium dioxide present in the sponge. The greater activity is indicated by the synergistic effect of greater adsorption, followed by photocatalytic studies. The titanium dioxide-polydimethylsiloxane

exhibited a lower reusability of three cycles in comparison with other catalytic sponges.

The silver bromide-silver chloride/silver melamine sponges were developed via immobilization of silver nanowires on the melamine sponge network, shifts silver into silver bromide-silver chloride, and the metallic silver is yielded by reduction reaction. The photocatalytic studies proved that the developed system is capable of removing Methyl Orange, Acid Orange 7, Malachite Green, Fuchsin Basic, Rhodamine B, and antibiotic sulfadiazine effectively. The improved separation of electron-hole pairs and visible light activity is ascribed to the enhanced catalytic activity of sponges (Kong et al. 2019). Zhang et al. (2023) discussed the superior role of reduced graphene oxide/carbon nitride composite sponge toward the effective removal of Methylene Blue (99%) and Rhodamine B (91%) in 180 min of visible light irradiation. The composite sponge also displayed a maximum reusability of five cycles. Figure 5 discusses the photocatalytic degradation mechanism of reduced graphene oxide/carbon nitride composite sponge toward dye removal. The superoxide and hydroxyl radicals are found to be the dominant radical species that aided the dye degradation.

Liang et al. (2021a) developed a porous ternary graphitic carbon nitride ($g\text{-C}_3\text{N}_4$)/bismuth tungstate (Bi_2WO_6)/molybdenum sulfide (MoS_2) heterojunction through a facile strategy for the removal of antibiotics. The combination of bismuth tungstate with graphitic carbon nitride was beneficial in the tuning of the morphology. The unique morphology prevented the heterojunction from the agglomeration and exhibited phenomenal light absorption with a large number of active sites. The ternary heterojunction exhibited a maximum surface area of $3794 \text{ m}^2 \text{ g}^{-1}$. The photocatalytic degradation studies claimed a 99% removal of sulfamethoxazole within one hour under visible light illumination with a reusability of six cycles. The superoxide radicals and holes were responsible for sulfamethoxazole redemption. The formation of heterojunction also prevented the recombination of charge carriers and enhanced the separation efficiency.

Lee et al. (2020) prepared a floating porous polydimethylsiloxane-titanium dioxide (TiO_2)-gold composite sponge for the elimination of dye. The titanium dioxide and gold nanoparticles are immobilized on the surface of interconnected pores of polydimethylsiloxane to yield a three-dimensional structure. The preparation was achieved using the sugar template method with titanium dioxide and in situ reduction of gold particles. The location of gold particles on the pores enhances the intimate contact between the titanium and boosts up the plasmonic photocatalysis. Under the illumination of ultraviolet light, the composite sponge exhibited a 1.8 times greater removal rate than the titanium dioxide sponge with a reusability of four cycles. However, because of the Schottky effect and

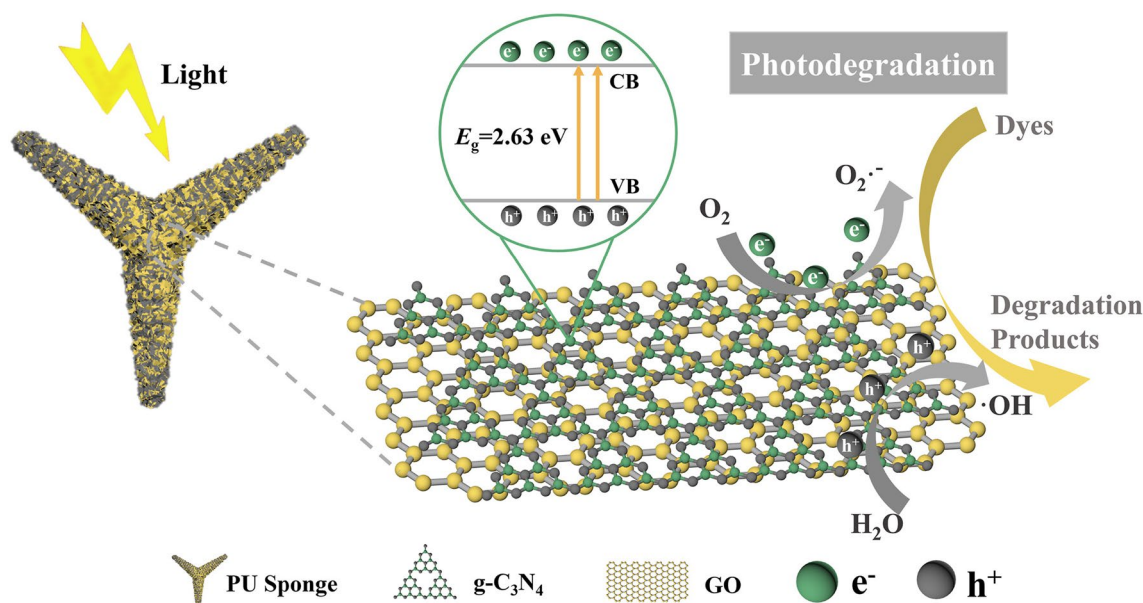


Fig. 5 Photocatalytic reclamation mechanism of dyes using reduced graphene oxide/carbon nitride (g-C₃N₄) composite sponge under visible light irradiation. Upon the illumination of visible light, the electrons move from the valence band of the carbon nitride (g-C₃N₄) to the conduction band. The free electrons will reduce oxygen to superoxide radicals, which effectively decompose the pollutants into car-

bon dioxide and water. Reprinted with permission of Elsevier from reference (Zhang et al. 2023). g-C₃N₄ is graphitic carbon nitride, PU is polyurethane, GO is reduced graphene oxide, CB is the conduction band, VB is the valence band, e⁻ is electrons, h⁺ is holes, E_g is band gap, O₂ is oxygen, and O₂⁻ is superoxide radicals

plasmonic effect, visible light is reported to have a better removal efficiency than ultraviolet light. The synergistic interaction between gold and titanium dioxide also played a vital role in the photocatalytic degradation of Rhodamine B.

Zhou et al. (2023) prepared the photocatalytic bismuth oxybromide (BiOBr)/sodium alginate/cellulose-based sponges for the removal of dye. The prepared hybrid photocatalytic sponges demonstrated 96% Rhodamine B removal in 90 min under the illumination of a 300-W xenon lamp. The presence of bismuth oxybromide (BiOBr) on the sponge surface improved photocatalytic properties and enhanced the flotation properties of sponges, resulting in enhanced reusability of five cycles. Later, the deposition of silver/silver chloride (AgCl) photocatalysts on the surface of a polydopamine-modified melamine sponge-assisted photocatalytic microreactor was developed against the removal of Methylene Blue. The Methylene Blue was completely degraded in 10 min under visible light irradiation. The main advantages of the microreactor are higher surface area, quick mass transfer, ease of operation, and low safety concerns (Duan et al. 2023).

Different from dyes, pharmaceuticals are emerging contaminants in water bodies that potentially cause severe hazards, including bioaccumulation and severe health problems (Balakrishnan et al. 2023c). Liu et al. (2021) emphasized the highly stable polyurethane sponges supported by tin-zinc oxide for the visible light degradation

of the tetracycline. The sponge photocatalyst was fabricated via in situ growth of tin-doped zinc oxide on the surface matrix of polydopamine-modified polyurethane through a double template-assisted bionic mineralization strategy. The degradation studied reported 96% elimination of tetracycline in 120 min with a total organic carbon removal of 42%. The effective contact between the photocatalyst and polymer matrix leads to the abundant availability of active sites and promotes light absorption from the ultraviolet region to the visible region. Further, the unique structure promoted the transfer of charge species, minimized the defects, and protected the catalyst from corrosion. The sponges also retained 91% removal efficiency even after five cycles, indicating good photo-stability of polyurethane sponges supported tin-zinc oxide sponges.

The melamine sponge@covalent framework composites were proposed by a team of researchers led by Lin et al. (2022a) for the removal of tetracycline using visible irradiation. The one-pot preparation method via reactive seeding strategy was adopted for the preparation of effective sponges. The one-pot preparation pathway ensures uniform and regular growth of covalent organic frameworks on the melamine sponges. About 97% of tetracycline removal efficiency is reported under visible light. The melamine sponge@covalent organic framework retained 94% removal efficiency after the 10th cycle. The phenomenal activity is ascribed to the reduction in the band gap of the sponges from

4.41 eV for melamine sponge to 2.76 eV for hybrid sponges, which enabled effective utilization of visible light. The highly porous and well-connected structure also enhanced the absorption of sunlight and minimized the scattering of light effectively. The hydroxyl radicals and superoxide radicals are prominent groups that play a vital role in the elimination of tetracycline.

Gao et al. (2022b) reported the three-dimensional ligno-sulfonate-based sponges impregnated with bismuth vanadate (BiVO_4)/polyaniline/silver photocatalyst for the effective removal of fluoroquinolones from water. Experimental studies reported 90% removal in batch mode (two hours) and 80% in continuous mode within thirty hours. The process of adsorption followed by photocatalysis is dependent on the surface degradation connected with effective adsorption because of plenty of acidic functional groups. The mechanistic studies proved that the sponge is a type-II heterojunction, enhancing the utilization of visible light and separation efficiency. The holes were found to be the highly active species that took part in photocatalytic degradation. Composite sponges are an effective self-purification system that is environmentally viable, has a lower price, and is highly efficient (Gao et al. 2022b). A highly elastic blocky catalyst was developed via proper growth and distribution of cobalt-manganese bimetallic oxide inside sponges (CoMnO_x @sponge) for the activation of peroxymonosulfate. The catalytic system completely removed the sulfonamide antibiotics within five minutes and followed a pseudo-first-order reaction. The blocky catalyst exhibited the phenomenal reusability of twenty cycles and could retain 90% efficiency (Jiang et al. 2022).

Table 3 summarizes different photocatalytic sponges used in the removal of noxious pollutants present in wastewater. Overall, photocatalytic sponges are highly versatile materials for the elimination of noxious compounds due to (i) highly porous three-dimensional interconnected structure, (ii) tuned band gap of the photocatalyst, (iii) easiness in the recovery of the photocatalyst with no mass loss, (iv) higher reusability, (v) elasticity, durability, and ability to form any shapes, (vi) easy to scale up and commercialize. However, the reactors must be constructed with the intention of scaling up for industry or any other practical uses in order to develop an appropriate photocatalytic reactor for photocatalytic sponges. Special focus must be given to the preparation of Z-scheme sponges to decrease the problems of the recombination of electron–hole pairs.

Disinfection

Microbial contamination has always posed a serious health risk to humans. The bacteria, fungi, algae, and viruses potentially cause eco-toxicity and different diseases to both man and animals (Yu et al. 2019; Balakrishnan et al. 2023a).

Thus, the photocatalytic disinfection strategy gathered research importance because of the higher disinfection efficiency and energy conversion of sponges (Wang et al. 2021). The photocatalytic bacterial and algal degradation is achieved via a strong radicals-assisted oxidation process. The illumination of a suitable light source on the photocatalyst surface tends to move the electrons from the valence band to the conduction band with the simultaneous formation of holes. These holes will directly attack the radical species on the surface of microorganisms and hinder the growth of organisms (Chinthala et al. 2021). The heat produced by photocatalytic degradation can also contribute toward the denaturation of proteins and kill the germs.

Recently, Li et al. (2022b) used melamine sponge-functionalized carbon nitride for the inactivation of *Staphylococcus aureus* and *Salmonella typhimurium*. The photo-studies proved that the carbon doping and nitrogen vacancies improved light absorption and increased the production of holes in photocatalysis. The photocatalytic performance of the melamine-functionalized carbon nitride sponge ensured the inactivation of *Staphylococcus aureus* and *Salmonella typhimurium*, respectively. The illumination of visible light and holes is generated in the valence band. These holes acted on the bacteria's surface and restricted the growth. The photocatalyst also produced heat under visible light, which increased the temperature of the water. The high temperature of the water is capable of destroying the proteins and destroying the germs.

Tu et al. (2021) emphasized self-supported reduced graphene oxide/bismuth oxybromide (BiOBr) composite on loofah sponge as a floating monolithic photocatalyst for the inactivation of microcystis aeruginosa seen in wastewater. The reduced graphene oxide acted as a binder to strengthen the interaction between the loofah and active catalytic material to speed up the charge transfer. Experimental studies reported more than 90% removal of microcystis aeruginosa, and the total organic carbon removal was 74% at the end of three hours. The good photocatalytic activity is ascribed to the formation of heterojunction between reduced graphene oxide and bismuth oxybromide. The catalytic sponge exhibited a reusability of five cycles with any decay, indicating the structural stability of the sponge.

The visible light-induced silver molybdate/terephthalic acid-functionalized carbon nitride loofah floating photocatalyst composites were developed to destroy the *Microcystis aeruginosa* through an oscillatory impregnation route. The composite sponge completely removed chlorophyll within four hours of visible light exposure. The silver molybdate/terephthalic acid-functionalized carbon nitride loofah floating photocatalyst exhibiting a reusability of five cycles with a decline of 8% is ascribed to the occupation of remaining algae or organic matter into the floating surface. Studies show that the algal cells became shriveled, and the

Table 3 Photocatalytic efficiency and cycles of reuse of the different photocatalytic sponges employed for wastewater remediation

Photocatalyst	Pollutant	Light source	Efficiency	Cycles of reuse	References
Titanium dioxide sponge composites	2,4,6-Trichlorophenol (20 mg L ⁻¹)	Light-emitting diode lamp	81% in 240 min	Not reported	Zhao et al. (2020)
Zeolitic Imidazole Framework-8-derived Zinc oxide/reduced graphene oxide/carbon sponge	Rhodamine B (10 mg L ⁻¹)	300-W Xenon lamp	99% in 120 min	3	Su et al. (2018)
Titanium dioxide with surface phase junction	Rhodamine B	Not reported	53% total organic carbon removal	5	Jiang et al. (2021)
Gold/zinc oxide/polyurethane	Rhodamine B (5 mg L ⁻¹)	300-W Xenon lamp	96% in 90 min	5	She et al. (2018)
Zinc oxide/polydimethylsiloxane	Methylene Blue (5 mg L ⁻¹)	4-W ultraviolet lamp	93%	10	Hossain et al. (2020)
Molybdenum oxide-octadecylamine-ferrous oxide polyurethane sponge	Methylene Blue (40 mg L ⁻¹)	Not reported	About 90% in 25 min	Not reported	Sui et al. (2021)
Titanium dioxide carbon nanotube sponge	Rhodamine B (1 × 10 ⁻⁵ mol L ⁻¹)	350-W Xenon lamp	About 80%	Not reported	Peng et al. (2015)
Wood-derived fiber bismuth oxybromide/silver bromide sponges	Rhodamine B (5 mg L ⁻¹)	Xenon lamp	99%	5	Xu et al. (2019)
Zinc oxide tetrapod sponges	Methylene Blue (5 mg L ⁻¹)	100-W ultraviolet lamp	96% in 130 min	Not reported	Lee et al. (2023)
	Methyl Orange (30 mg L ⁻¹)		61% in 130 min	Not reported	
Red phosphorous/silver sponge monolith	Rhodamine 6G (20 mg L ⁻¹)	300-W Xenon lamp	82% in 180 min	5	Wang et al. (2018b)
Gadolinium-doped vanadium oxide/Mxene	Methylene blue (5 mg L ⁻¹)	Sunlight	92% in 120 min	5	Tahir et al. (2022)
Polyvinyl alcohol sponge-loaded bismuth tungstate	Tetracycline (70 mg L ⁻¹)	500-W Xenon lamp	94% in 120 min	4	Zhang et al. (2016a)
3D bombax-structured carbon nanotube sponge coupled with silver phosphate	Tetracycline (10 mg L ⁻¹)	300-W Xenon lamp	90% in 60 min	5	Jin et al. (2019)
Collagen-titanium dioxide nanobio-sponge	Rhodamine B (0.03 M)	200-W medium pressure mercury lamp	95% in 130 min	3	Nagaraj et al. (2021)
Three-dimensional sponge-silver tetrasilicate microblock	Methylene Blue (20 mg L ⁻¹)	300-W Xenon lamp	98% in 30 min	4	Li et al. (2022a)
Sponge-loaded Bismuth tungstate/zinc ferrite	Tetracycline (5 mg L ⁻¹)	500-W Xenon lamp	98% in 90 min	4	Zhang et al. (2017a)
Monolithic microreactor with silver/silver chloride coated on polydopamine-modified melamine sponge	Methylene Blue (10 mg L ⁻¹)	300-W Xenon lamp	99% in 15 min	5	Cardil et al. (2021)
Reduced graphene oxide/carbon nitride composite sponge	Methylene Blue (10 mg L ⁻¹) Rhodamine B (10 mg L ⁻¹)	Sun irradiation	99% in 180 min 91% in 180 min	5	Zhang et al. (2023)

Table 3 (continued)

Photocatalyst	Pollutant	Light source	Efficiency	Cycles of reuse	References
Zinc oxide tetrapod sponges	Methylene blue (5 mg L ⁻¹)	100-W ultraviolet lamp	96% in 130 min	Not reported	Lee et al. (2023)
Sodium bismuth sulfide chitosan cellulose sponges	Methylene blue (30 mg L ⁻¹)	300-W Xenon lamp	98% in 60 min	5	Liu et al. (2023a)

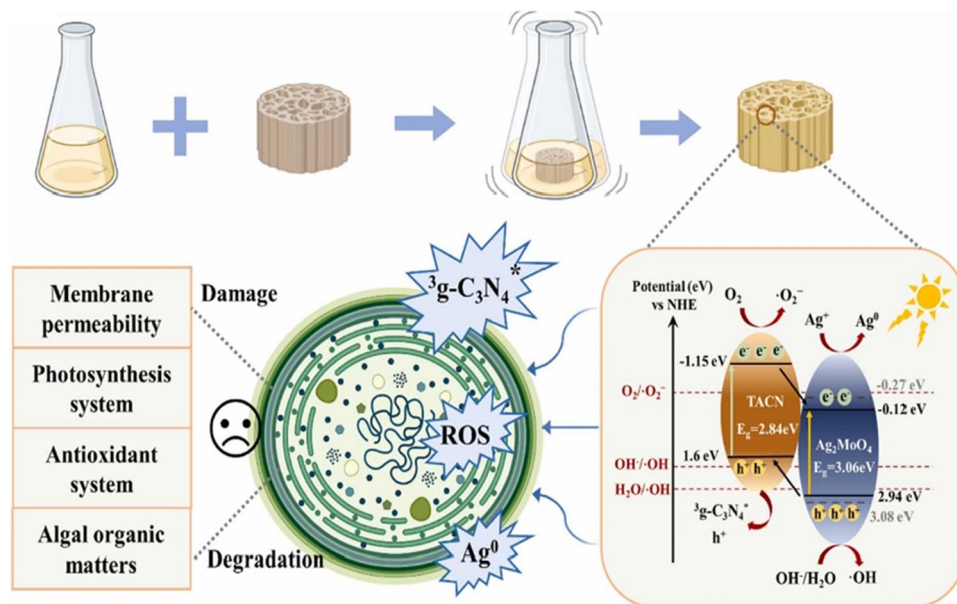


Fig. 6 Photocatalytic inactivation of *Microcystis aeruginosa* using silver molybdate (Ag_2MoO_4)/terephthalic acid-functionalized carbon nitride@loofah sponge photocatalyst. The reactive oxygen species, zero-valent silver ions, and triplet excited state of carbon nitride are generated under the illumination of visible light. The proper contact between the generated species and the algal cells degraded the cell wall and cell membrane of algae. The destruction of cell walls destroyed membrane permeability and antioxidant systems. At last,

the micro-organisms are inactivated. Reprinted with permission of Elsevier from reference (Fan et al. 2023). Ag_2MoO_4 is silver molybdate, TACN is terephthalic acid-functionalized carbon nitride, ROS is reactive oxygen species, NHE is normal hydrogen electrode, h^+ is hole, e^- is electron, Ag^+ is silver ions, Ag^0 is zero-valent silver, $^3\text{g-C}_3\text{N}_4^*$ is triplet excited state of carbon nitride, and E_g is band gap, $\text{O}_2^{\cdot-}$ is superoxide radicals, $\text{OH}^{\cdot-}$ is hydroxyl radicals, OH^- is hydroxyl ions, O_2 is oxygen, and H_2O is water

Table 4 Photocatalytic sponges employed for disinfection of micro-organisms present in wastewater

Photocatalyst	Organism	Light source	Efficiency	References
Black melamine-based sponge	Salmonella	300-W xenon lamp	98% in 40 min	Li et al. (2020)
Encapsulated zinc/cobalt nanocrystals into sponge porous carbon	<i>Escherichia Coli</i>	Visible light	72% adenosine triphosphate of <i>E.Coli</i> is reduced	Bai et al. (2022)
Silver carbonate-Nitrogen/graphene oxide/polyurethane sponge	<i>Microcystis aeruginosa</i>	Visible light	100% of chlorophyll removal in 300 min	Fan et al. (2020)
Graphitic carbon nitride- bismuth molybdate/silver iodide floating sponge	<i>Microcystis aeruginosa</i>	Visible light	100% removal of algae cells in 360 min	Sun et al. (2022)
Nitrogen, sulfur-carbon quantum dots/ Bismuth molybdate/titanium dioxide	<i>Bacillus Subtilis</i> <i>Escherichia Coli</i>	Visible light	Not reported	Qu et al. (2020)

cell boundaries became more irregular after 90 min. The destruction of cell walls and membranes affirms the disruption of algal cells via the rupture of internal structure. The photocatalytic inactivation of *Microcystis aeruginosa* using the floating photocatalyst under visible light is reported in Fig. 6. The hybrid sponge could easily produce reactive oxygen species, zero-valent silver, and carbon nitride under the influence of visible light, which will interact with algal cells via floating properties. Later, the cell wall is destroyed, followed by the complete damage of membrane permeability, photosynthetic systems, anti-oxidation systems, and algae, which are inactivated (Fan et al. 2023).

Photocatalytic sterilization is an effective tool in the elimination of viruses, pathogens, and algae seen in water sources, as given in Table 4. The three-dimensional sponges exhibited phenomenal performance due to easiness in recovery and reusability. However, further studies are pre-requisite to assess the maximum life of the sponges. The photo-stability of the sponges must be confirmed using scanning electron microscopy, X-ray diffraction, and Fourier transform infrared analysis. Detailed studies are necessary on the fundamental interaction between sponge and bacteria, including the photo-generated reactive oxygen species' antibacterial behavior and the interface reactions that must be elucidated. The integration of photocatalysis with other advanced oxidation processes (ozonation and Fenton's) helps to enhance the removal efficiency by improving visible light utilization.

Photocatalytic reaction

The photocatalytic sponge is also used as an efficient catalyst for the smooth conduction of chemical reactions. Zhang et al. (2017b) fabricated highly bi-functional organic sponges as a photocatalyst for the coupling of tertiary amines with ketones in water under the illumination of visible light. Polydimethylsiloxane is elected as an efficient aid for sponges due to stability and transparency. The sponges are efficiently developed via polymer surface modification and solid-phase peptide synthesis. The scanning electron microscopy studies showed that the prepared material is a three-dimensional porous structure. The catalytic activity was tested using the cross-dehydrogenative coupling reaction among N-phenyltetrahydroisoquinoline and acetone. Studies proved that the sponges were able to catalyze the asymmetric transformations with phenomenal enantioselectivity (highest yield = 93%). The sponges also exhibited a yield of 87% after the tenth consecutive cycle. The study provides insights into easy catalyst preparation, separation, easy recyclability, and ability to scale up.

Yao et al. (2022) prepared a three-dimensional hierarchical porous ultrathin loofah-carbon nitride (C_3N_4) sponge through supramolecular pre-organization coupling assisted with an oxidation etching process, where oxygen and nitrogen atom vacancies are developed. Brunauer–Emmett–Teller surface area of the loofah-carbon

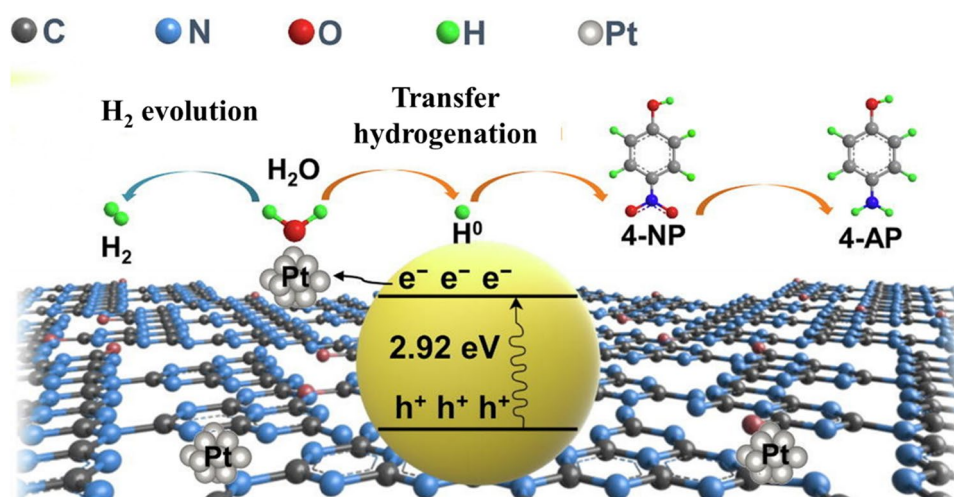


Fig. 7 Schematic representation of the photocatalytic transfer hydrogenation and hydrogen evolution using loofah-carbon nitride sponge. The three-dimensional sponge morphology and the oxygen doped enhanced the surface area, visible light utilization, and hydrophilicity. The loofah-carbon nitride sponge acted as a reliable light and water absorber. Further, platinum nanoclusters behaved as an efficient medium for the transfer of electrons. These characteristic properties helped in the conversion of nitrophenol to 4-aminophenol through a reaction between the absorbed water. The photo-induced electrons

undergo a reaction with water molecules to yield photo-generated hydrogen species and 4-aminophenols. In the absence of nitrophenols, the photo-induced electrons directly reduce water to photo-generated hydrogen species and hydrogen. Reprinted with permission from Elsevier from reference (Yao et al. 2022). C is carbon, N is nitrogen, O is oxygen, H is hydrogen, Pt is platinum, H₂ is hydrogen, H⁰ is photo-generated hydrogen species, 4-NP is 4-nitrophenol, 4-AP is 4-aminophenol, e⁻ is electrons, and h⁺ is holes

nitride sponge is $208 \text{ m}^2 \text{ g}^{-1}$, which is almost 61 times greater than bulk carbon nitride. The increased surface area is beneficial in efficient light harvesting. The experimental studies reported a 96% hydrogenation of 4-nitrophenol. From Fig. 7, it is evident that nitrophenol is converted to aminophenol through the effective reaction between the water and absorbed water. The loofah-carbon nitride sponge is an effective material, but no studies have reported on its recyclability and stability.

Photocatalytic hydrogen evolution

The energy crisis is one of the most trending global issues that urges the research community to produce clean energy efficiently. The complete exploration of clean and renewable solar energy is necessary to minimize the impact of greenhouse gases and to secure the energy demand for the future (Reddy et al. 2018). Photocatalytic hydrogen evolution is a sustainable and economical pathway to developing a resilient hydrogen economy.

Zhan et al. (2022) emphasized the pyridazine-doped graphitic carbon nitride ($\text{g-C}_3\text{N}_4$) with nitrogen defects and spongy structure for photocatalytic water splitting. The experimental studies reported a maximum hydrogen production of $11 \text{ mmol h}^{-1} \text{ g}^{-1}$, which is 94 times higher than bare carbon nitride. The higher efficiency of photocatalyst is indicated by the (i) formation of nitrogen defects between adjacent tri-s-triazine groups, (ii) effective migration of charge carriers and higher separation efficiency, and (iii) spongy structure offers several numbers of amino groups. The loofah-carbon nitride sponge exhibited a photocatalytic evolution of $4.8 \text{ mmol h}^{-1} \text{ g}^{-1}$, which is 26 times greater than bulk carbon nitride by using platinum as a co-catalyst. The photocatalytic sponge also exhibited recyclability for twenty hours with a minor decline in activity. The results confirmed the stability of the loofah-carbon nitride sponge because of hierarchical porous, and the calculated quantum efficiency of the hydrogen evolution is found to be 10% at 420 nm. The photo-induced electrons directly reduce water to photo-generated hydrogen species and hydrogen, as indicated in Fig. 7 (Yao et al. 2022).

Wang et al. (2019) focused on a carbon nitride sponge developed via green and environmentally free methods using melamine and nucleobases as chief starting material. The prepared catalyst exhibited a higher hydrogen generation of $5 \text{ mmol h}^{-1} \text{ g}^{-1}$ using 10% triethanolamine as a sacrificial reagent under 300-W Xenon lamp. The prepared catalyst also exhibited a reusability of four cycles and showed no prominent change in X-ray diffraction spectra before and after the study. The steric hindrance and molecular activity of nucleobases possess potential influence on catalyst activity. The excellent catalytic activity is indicated by (i) the higher surface area of $127 \text{ m}^2 \text{ g}^{-1}$, (ii) good biocompatibility

and hydrogen bonding tendency of nucleobase provided multiple binding sites for the catalyst, (iii) reduced recombination of electron–hole pairs and improved light absorption (band gap = 2.65 eV).

The zeolitic imidazole framework-8 (ZIF-8)/zinc oxide (ZnO) nanocages/reduced graphene oxide/carbon sponge was developed by a team of researchers led by Su et al. (2018) toward hydrogen evolution reaction (Su et al. 2018). The photocatalytic studies claimed an improved hydrogen generation of $0.073 \text{ mmol g}^{-1}$ using 25% methanol as a sacrificial reagent under 300-W xenon lamp (catalyst loading = 50 mg). The enhancement in hydrogen generation is seen upon the introduction of reduced graphene oxide, which minimized the recombination of electron–hole pairs ($0.067 \text{ mmol g}^{-1}$) and exhibited a reusability of three cycles. The better catalytic activity is due to the porous structure and higher surface area ($7.46 \text{ m}^2 \text{ g}^{-1}$) of the sponge, which provides an effective place for the diffusion of reactants. The enhancement in the optical property (2.84 eV) of the catalyst improved visible light utilization.

Liang et al. (2015) developed three-dimensional graphitic carbon nitride monoliths, which were capable of generating hydrogen under visible light irradiation. The prepared three-dimensional graphitic carbon nitride exhibited 2.84 times higher catalytic activity than pristine graphitic carbon nitride under visible light. The three-dimensional porous networks, higher surface area, higher visible light utilization, and greater separation efficiency lead to phenomenal catalytic activity. Wang et al. (2018a) reported a maximum hydrogen evolution of $31.95 \text{ } \mu\text{mol}$ for nitrogen-defect-carbon nitride ($\text{g-C}_3\text{N}_{x(0.1)}$)/nickel-selenide and $95.0 \text{ } \mu\text{mol}$ for nitrogen-defect $\text{g-C}_3\text{N}_{x(0.1)}$ /platinum (Pt) under visible light. The presence of nitrogen defects enhanced visible light harvesting and improved the separation of charge carriers, leading to phenomenal catalytic activity.

Zhang et al. (2016b) reported the facile preparation of graphene sponge from graphene oxide exhibited a maximum hydrogen evolution of $361 \text{ } \mu\text{mol}$, which is 28 times greater than that of pristine graphene oxide. The maximum apparent quantum yield of 75% is observed at a wavelength of 420 nm. Highly flexible porous melamine formaldehyde carbon sponge material coated with graphitic carbon nitride was developed using fast calcination of melamine–formaldehyde foam. The prepared affordable sponge is composed of a three-dimensional interconnected graphitic carbon network exhibiting a highly mesoporous structure and a mechanical strength of 26 MPa. The hybrid sponge exhibited the photocatalytic hydrogen evolution of $2.1 \text{ mmol h}^{-1} \text{ g}^{-1}$, which is almost 15 times greater than that of pristine graphitic carbon nitride. The hybrid sponges also exhibited a reusability of four cycles (Kang et al. 2022).

The limited number of studies indicates that photocatalytic hydrogen production using sponges is in the initial stages. Studies have proved that the higher flexibility, efficiency, and reusability of photocatalysts in water splitting make them unique from powdered nanocatalysts. The three-dimensional structure also contributed to the greater number of active sites and made the recovery and reuse easier. However, further research is necessary to overcome the following challenges: Firstly, understanding the kinetics of photocatalytic water splitting is pre-essential. The low-cost alternatives for deposition agents (gold and platinum) on sponges must be figured out without compromising quantum yield. Secondly, from the engineering point of view, highly expensive dopants and sacrificial agents are employed in deionized water to generate hydrogen gas. A standard protocol for the selection of the sacrificial agent and the respective concentration is necessary. Finally, in the modern world, the computational modeling of photocatalytic sponges will help in the development of efficient sponges with abundant active sites, surface area, porosity, and minimized recombination.

Carbon dioxide reduction

The continuous dependence and exploration of fossil fuels end up in the emission of tons of carbon dioxide into the atmosphere and are responsible for global warming. In 2017, about 32.8 billion tons of CO₂ was discharged into the environment, and this will continue to increase in the near future. Studies also indicated a hike in global temperature by 2 °C by 2050 (Aggarwal et al. 2021). Thus, the emission of carbon dioxide into the environment must be reduced significantly. From the point of sustainable energy, the conversion of carbon dioxide into fuels using visible light is a prominent solution to overcome the limited supply of fossil fuels (Wen et al. 2017). The photocatalytic conversion of carbon dioxide into fuels is an effective strategy for tackling environmental problems.

Lin et al. (2022b) developed amphiphilic cobalt oxide biochar for the photocatalytic reduction of carbon dioxide into other chemicals. The amphiphilic performance of the cobalt oxide-biochar is ascribed to micro- or nanostructure arising from the loofah sponge and cobalt oxide. The experimental studies reported the production of carbon monoxide at the rate of 48.3 μmol h⁻¹ with a reusability of four cycles. The carbon monoxide production efficiency of the photocatalyst is also consistent with the absorption of the photosensitizer, where performance declines with increment in wavelength. Studies claimed that the charge migration efficiency between the catalyst and carbon dioxide enhanced the carbon dioxide conversion. The carbon dioxide mass transfer also exhibited a prominent role in carbon dioxide conversion. Further, undulating folds derived from the sponges

contained several microstructures responsible for the surface roughness of the photocatalyst (Lin et al. 2022b).

Yang et al. (2018) reported that the recyclable monolithic graphitic carbon nitride/melamine sponge used an ultrasonic coating strategy. The photocatalytic studies reported the carbon dioxide reduction into carbon monoxide (7.48 μmol h⁻¹ g⁻¹) and methane (3.93 μmol h⁻¹ g⁻¹), respectively. The predominant catalytic activity of the monolithic sponges is due to the inherent porous structure of melamine along with the greater surface area (7.6 m² g⁻¹) than the corresponding pristine form (0.9 m² g⁻¹). The higher surface area leads to abundant availability of active sites. The optical studies also proved higher visible light harvesting through the decline in the band gap of the hybrid sponge to 2.79 eV, which reduced the recombination of the electron–hole pairs. So, the graphitic carbon nitride (g-C₃N₄) melamine sponge is a versatile material for carbon dioxide reduction due to the high elasticity, firmness, mechanical strength, and photostability of sponges (Yang et al. 2018).

Zhang et al. (2018) reported graphitic carbon nitride (g-C₃N₄)/graphene oxide-wrapped sponge monoliths to produce carbon monoxide, methane, and hydrogen of 42.9, 4.6, and 1.6 μmol h⁻¹ g⁻¹, which is higher than graphitic carbon nitride/graphene oxide composites. The synergistic effect of graphene oxide and melamine sponge makes the hybrid composites possess a higher surface area. Upon the absorption of light sources, electrons and holes are excited, and the reactants are firstly adsorbed on the photocatalyst surface. The synergistic interaction between the graphene oxide and melamine sponge is observed during the initial period. The transfer of photogenerated electrons and holes toward the surface of the catalyst effectively reduces carbon dioxide. The higher conductivity of the graphene oxides supplies electrons abundantly to avoid the recombination of charge carriers. The visible light absorption is improved through the surface sensitization of graphene oxide. The photogenerated electrons and holes reduce the carbon dioxide to chemicals.

Wang et al. (2023) developed biomimetic porphyrin-modified three-dimensional porous material porphyrin-loaded ammonia-treated carbonized zinc-cobalt-zeolitic imidazole framework-carbon nitride. The experimental studies reported the superior catalytic activity leads to the conversion of carbon dioxide into methane (34.5 μmol g⁻¹) and carbon monoxide (392.2 μmol g⁻¹) with a reusability of four cycles. The photoinduced electron–hole pairs followed the typical type-II pathways, the presence of porphyrin structure, and the higher conductivity of the zeolitic imidazole framework materials accelerated the rapid movement of photogenerated electrons and enhanced the carbon dioxide sequestration.

Later, Yang et al. (2022) developed a hierarchically porous deficient nickel carbonate embedded sponge magnesium calcite disclosed photocatalyst for the reduction of

carbon dioxide into carbon monoxide ($10.5 \mu\text{mol h}^{-1} \text{g}^{-1}$). The experimental studies proved that the carbonate vacancy created in the nickel carbonate improved the adsorption and followed by the activation of carbon dioxide than the O-vacant nickel carbonate. The carbon dioxide molecule is easily deformed on the surface of nickel carbonate and activated to the formation of an intermediate during the reactions. The study showcases the role of defect materials in the photocatalytic reduction of carbon dioxide. Wang et al. (2014) developed a three-dimensional macro/mesoporous titanium dioxide (TiO_2) sponge via gelation of lotus root starch for the reduction of carbon dioxide. The experimental studies reported that titanium dioxide sponge exhibited 2.6 times greater carbon dioxide conversion to methane than that of titanium dioxide. The phenomenal activity of the sponge photocatalyst is attributed to three reasons: (i) The macroporous structure supports the gas diffusion of reactants and products, (ii) the promotion of the multiple-reflection effect inside the microcavities enables the visible light harvesting for the higher duration and ensures efficient light absorption, (iii) the mesoporous structure improves the gas capture/adsorption of reactants and ensures the availability of more active sites.

The high porosity and surface area make the photocatalytic sponges suitable for the photocatalytic reduction of carbon dioxide. Continuing research is necessary to figure out the main drawbacks of sponges in carbon dioxide reduction. Studies reported a lower conversion rate of carbon dioxide into chemicals, which is ascribed to a lower utilization of visible light and a recombination of electron–hole pairs. Further, studies are mandatory to understand the fundamental mechanism behind the conversion of carbon dioxide. The isotope labeling analysis using isotope carbon dioxide as a reactant is useful in affirming the obtained products from the photofixation of carbon dioxide.

Perspective

The applications of photocatalytic sponges must be further explored based on the optimization of photocatalytic activity and the compatibility of sponges. The following points must be considered to develop highly efficient photocatalytic sponges for environmental remediation.

- Current research on the structural tuning of the photocatalyst that is present on sponges is insufficient. For the effective interaction between the photocatalyst and sponge, special emphasis must be given to the functional group, and size distribution and porosity on the sponge performance must be explored. The modification of the photocatalysts using other functional materials (for example, metal–organic frameworks) can be used to enhance the adsorption, catalytic properties, and stability of the sponges. The design of photocatalytic sponge heterojunctions is beneficial in resolving the problems associated with the recombination of electron–hole pairs, where the Z-scheme or S-scheme must be considered.
- The large-scale development of photocatalytic sponges is a major challenge that hinders practical applications. Researchers must focus on the development of a proper fabrication strategy for the enhancement of stability for prolonged operations in continuous mode. The preparation route must be affordable, environmentally friendly, and economically viable. The template-assisted methods using sugar or salt leaching methods are easy to scale up. Further, density functional theory calculations are beneficial in estimating the stability of the sponges.
- The complete mineralization of organic pollutants is very complex. So, a detailed understanding of intermediate products formed during the degradation process must be studied using mass spectroscopic techniques. Photocatalytic degradation studies are commonly conducted using distilled water, so the conduction of photostudies using real wastewater is necessary to understand the capability of photocatalytic sponges.
- Next, the photocatalytic degradation mechanism of photocatalytic sponges needs more clarity. Many debates have arisen as a result of these uncertainties in the explanation of the photocatalytic efficacy of the sponges in various composites. A detailed study on photocatalytic sponges' mechanisms is mandatory, specifically for advanced in situ techniques.
- The total eradication of organic contaminants utilizing photocatalytic technology is difficult, just like other procedures. As a result, there is a bigger practical benefit when photocatalysis is combined with other cutting-edge oxidation processes, including photo-assisted Fenton's reaction, persulfate oxidation, and photoelectrocatalysis. The synergistic process generates radicals with high oxidation capacity and improves the photocatalytic degradation of organic pollutants. The kinetic matching between these techniques may attain greater research interest in the future.
- Most of the researchers have only conducted reusability studies up to five cycles. Detailed studies on the reusability of photocatalytic sponges are necessary to understand the saturation limit of sponges. The conduction of characterization using X-ray diffraction, Fourier transform infrared spectra, and scanning electron microscopy of used sponges is mandatory to predict the stability of sponges. Reusability is the prominent advantage of sponges, so that must be explored fully for different applications.

- The density functional theory helps to predict key information for hydrogen evolution and carbon dioxide reduction. For hydrogen generation applications, density functional theory is beneficial in providing scientific aspects on the surface reaction and interface charge transfer. The density functional theory can be adopted to understand the activation state of carbon dioxide.

Conclusion

We introduce photocatalytic sponges as a very adaptable material even though they have recently demonstrated significant uses in the environment and energy, despite the fact that sponges have been known for a decade. The development of photocatalytic sponges for energy production and environmental clean-up is summarized in the article. Different preparation routes adopted for the preparation of photocatalytic sponges are outlined in detail. Among them, dip-coating, freeze-drying, and template-assisted preparation routes are widely explored for different applications. The efficacy of the photocatalytic sponges was assessed through photocatalytic performance in organic pollutant removal, disinfection, hydrogen production, and carbon dioxide reduction into chemicals or fuels. The higher surface area, porosity, three-dimensional well-interconnected structures, ease of recovery, and reusability make them suitable for photocatalytic technology. Finally, the perspectives of the three-dimensional photocatalytic sponges are elucidated.

Authors' contribution All authors contributed to the study's conception and design. Data collection and analysis were performed by AB, MMJ, ND, and MC. The first draft of the manuscript was written by AB, MMJ, and ND. MP, D-VNV, and MC reviewed and edited the manuscript. All authors read and approved the final manuscript. D-VNV declares that he is an Editor of Environmental Chemistry Letters.

Funding The authors declare that no funds, grants, or other supports were received during the preparation of this manuscript.

Declarations

Conflict of interest The authors have no relevant financial or non-financial interests to disclose.

References

- Abdelhafeez IA, Zhou X, Yao Q, Yu Z, Gong Y, Chen J (2020) Multifunctional edge-activated carbon nitride nanosheet-wrapped polydimethylsiloxane sponge skeleton for selective oil absorption and photocatalysis. *ACS Omega* 5:4181–4190. <https://doi.org/10.1021/acsomega.9b03994>
- Aggarwal M, Basu S, Shetti NP, Nadagouda MN, Kwon EE, Park YK, Aminabhavi TM (2021) Photocatalytic carbon dioxide reduction: exploring the role of ultrathin 2D graphitic carbon nitride (g-C₃N₄). *Chem Eng J* 425:131402. <https://doi.org/10.1016/j.cej.2021.131402>
- Anderson TR, Hawkins E, Jones PD (2016) CO₂, the greenhouse effect and global warming: from the pioneering work of Arrhenius and Callendar to today's earth system models. *Endeavour* 40:178–187. <https://doi.org/10.1016/j.endeavour.2016.07.002>
- Bai Y, Shi C, Ma X, Li J, Chen S, Guo N, Yu X, Yang C, Zhang Z (2022) Encapsulation of Zn/Co nanocrystals into sponge-like 3D porous carbon for *Escherichia coli* inactivation coupled with ultrasound: characterization, kinetics and inactivation mechanism. *Chem Eng J* 447:137545. <https://doi.org/10.1016/J.CEJ.2022.137545>
- Balakrishnan A, Chinthala M (2022) Comprehensive review on advanced reusability of g-C₃N₄ based photocatalysts for the removal of organic pollutants. *Chemosphere*. <https://doi.org/10.1016/J.CHEMOSPHERE.2022.134190>
- Balakrishnan A, Chinthala M (2023) Effective sequestration of tetracycline from aqueous streams using metal-free chemically functionalized porous g-C₃N₄ ☆. *Environ Pollut* 333:122057. <https://doi.org/10.1016/j.envpol.2023.122057>
- Balakrishnan A, Appunni S, Chinthala M, Viet D (2022a) Biopolymer-supported TiO₂ as a sustainable photocatalyst for wastewater treatment : a review. *Environ Chem Lett*. <https://doi.org/10.1007/s10311-022-01443-8>
- Balakrishnan A, Chinthala M, Polagani R, Vo D-VN (2023a) Removal of tetracycline from wastewater using g-C₃N₄ based photocatalysts: a review. *Environ Res* 216:18–52. <https://doi.org/10.1016/j.envres.2022.114660>
- Balakrishnan A, Chinthala M, Polagani RK (2023b) 3D kaolinite/g-C₃N₄-alginate beads as an affordable and sustainable photocatalyst for wastewater remediation. *Carbohydr Polym*. <https://doi.org/10.1016/j.carbpol.2023.121420>
- Balakrishnan A, Kunnel ES, Sasidharan R, Chinthala M, Kumar A (2023c) 3D black g-C₃N₄ isotype heterojunction hydrogels as a sustainable photocatalyst for tetracycline degradation and H₂O₂ production. *Chem Eng J*. <https://doi.org/10.1016/j.cej.2023.146163>
- Balakrishnan A, Ponnuchamy M, Kapoor A (2022b) Emerging Contaminants in Wastewater and Associated Treatment Technologies, Springer International Publications
- Bazrafshan Z, Stylios GK (2019) Spinnability of collagen as a biomimetic material: a review. *Int J Biol Macromol* 129:693–705. <https://doi.org/10.1016/J.IJBIOMAC.2019.02.024>
- Cardil A, Monedero S, Schag G, Tapia M (2021) Efficient and stable monolithic microreactor with Ag/AgCl photocatalysts coated on polydopamine modified melamine sponge for photocatalytic water purification. *J Alloys Compd*. <https://doi.org/10.1016/j.cofsulfa.2022.130759>
- Chen Y, Hanshe M, Sun Z, Zhou Y, Mei C, Duan G, Zheng J, Shiju E, Jiang S (2022) Lightweight and anisotropic cellulose nanofibril/rectorite composite sponges for efficient dye adsorption and selective separation. *Int J Biol Macromol* 207:130–139. <https://doi.org/10.1016/J.IJBIOMAC.2022.03.011>
- Chinthala M, Balakrishnan A, Venkataraman P, Gowtham VM, Polagani RK (2021) Synthesis and applications of nano-MgO and composites for medicine, energy, and environmental remediation: a review. *Environ Chem Lett* 19:4415–4454. <https://doi.org/10.1007/s10311-021-01299-4>
- Duan J, Fang X, Li C, Qu J, Guo L, Zou Y, Xiang M, Wang W (2023) Efficient and stable monolithic microreactor with Ag/AgCl photocatalysts coated on polydopamine modified melamine sponge for photocatalytic water purification. *Colloids Surf A Physicochem Eng Asp* 659:130759. <https://doi.org/10.1016/j.cofsulfa.2022.130759>

- Fan G, Chen Z, Hong L, Du B, Yan Z, Zhan J, You Y, Ning R, Xiao H (2020) Simultaneous removal of harmful algal cells and toxins by a $\text{Ag}_2\text{CO}_3\text{-N:GO}$ photocatalyst coating under visible light. *Sci Total Environ* 741:140341. <https://doi.org/10.1016/j.scitotenv.2020.140341>
- Fan G, Cai C, Chen Z, Luo J, Du B, Yang S, Wu J (2023) Visible-light-driven self-floating $\text{Ag}_2\text{MoO}_4/\text{TACN@LF}$ photocatalyst inactivation of *Microcystis aeruginosa*: performance and mechanisms. *J Hazard Mater* 441:129932. <https://doi.org/10.1016/j.jhazmat.2022.129932>
- Fang Y, Huang Q, Liu P, Shi J, Xu G (2018) A facile dip-coating method for the preparation of separable MoS_2 sponges and their high-efficient adsorption behaviors of Rhodamine B. *Inorg Chem Front* 5:827–834. <https://doi.org/10.1039/c8qi00012c>
- Gao B, Pan Y, Yang H (2022a) Enhanced photo-Fenton degradation of fluoroquinolones in water assisted by a 3D composite sponge complexed with a S-scheme $\text{MoS}_2/\text{Bi}_2\text{S}_3/\text{BiVO}_4$ ternary photocatalyst. *Appl Catal B Environ* 315:121580. <https://doi.org/10.1016/j.apcatb.2022.121580>
- Gao B, Tao K, Xi Z, El-sayed MMH, Shoeib T, Yang H (2022b) Fabrication of 3D lignosulfonate composited sponges impregnated by $\text{BiVO}_4/\text{polyaniline}/\text{Ag}$ ternary photocatalyst for synergistic adsorption-photodegradation of fluoroquinolones in water. *Chem Eng J* 446:137282. <https://doi.org/10.1016/j.cej.2022.137282>
- Gao X, Ai L, Wang L, Ju Y, Liu S, Wang J (2022c) The stable and elastic graphitic carbon nitride/polyvinyl alcohol photocatalytic composite sponge: Simple synthesis and application for wastewater treatment. *J Environ Chem Eng* 10:107814. <https://doi.org/10.1016/j.jece.2022.107814>
- He X, Kai T, Ding P (2021) Heterojunction photocatalysts for degradation of the tetracycline antibiotic: a review. *Environ Chem Lett* 19:4563–4601. <https://doi.org/10.1007/s10311-021-01295-8>
- Hickman R, Walker E, Chowdhury S (2018) $\text{TiO}_2\text{-PDMS}$ composite sponge for adsorption and solar mediated photodegradation of dye pollutants. *J Water Process Eng* 24:74–82. <https://doi.org/10.1016/j.jwpe.2018.05.015>
- Hossain S, Chun DM (2020) ZnO decorated polydimethylsiloxane sponges as photocatalysts for effective removal of methylene blue dye. *Mater Chem Phys* 255:123589. <https://doi.org/10.1016/j.matchemphys.2020.123589>
- Islam MT, Rosales J, Saenz-Arana R, Kim H, Sultana KA, Lin Y, Villagram D, Noveron JC (2019) Synthesis of high surface area transition metal sponges and their catalytic properties. *New J Chem* 43:10045–10055. <https://doi.org/10.1039/c9nj02096a>
- Jbeli A, Ferraria AM, Botelho do Rego AM, Boufi S, Bouattour S (2018) Hybrid chitosan- TiO_2/ZnS prepared under mild conditions with visible-light driven photocatalytic activity. *Int J Biol Macromol* 116:1098–1104. <https://doi.org/10.1016/j.ijbiomac.2018.05.141>
- Jiang S, Agarwal S, Greiner A (2017) Low-density open cellular sponges as functional materials. *Angew Chemie Int Ed* 56:15520–15538. <https://doi.org/10.1002/anie.201700684>
- Jiang Y, Qin Y, Yu T, Lin S (2021) Synthesis of sponge-like TiO_2 with surface-phase junctions for enhanced visible-light photocatalytic performance. *Chin Chem Lett* 32:1823–1826. <https://doi.org/10.1016/j.ccllet.2020.11.010>
- Jiang ZR, Wang P, Zhou YX, Wang C, Jiang J, Lan Y, Chen C (2022) Fabrication of a 3D-blocky catalyst (CoMnOx@ sponge) via mooring Co-Mn bimetallic oxide on sponge to activate peroxy-monosulfate for convenient and efficient degradation of sulfonamide antibiotics. *Chem Eng J* 446:137306. <https://doi.org/10.1016/j.cej.2022.137306>
- Jin J, Liu M, Feng L, Wang H, Wang Y, Nguyen TAH, Wang Y, Lu J, Li Y, Bao M (2019) 3D Bombax-structured carbon nanotube sponge coupling with Ag_3PO_4 for tetracycline degradation under ultrasound and visible light irradiation. *Sci Total Environ* 695:133694. <https://doi.org/10.1016/j.scitotenv.2019.133694>
- Kakaei K, Esrafil MD, Ehsani A (2019) Graphene and anticorrosive properties. *Interface Sci Technol* 27:303–337. <https://doi.org/10.1016/B978-0-12-814523-4.00008-3>
- Kang S, Chen M, Wang Y, Tang F, Liu Y, Cui L, Dong M (2022) Engineering a 3D porous carbon sponge as a self-floating solar energy utilization platform for photothermal oil spill recovery and photocatalytic H_2 evolution. *Sustain Energy Fuels* 7:409–419. <https://doi.org/10.1039/d2se01463g>
- Kong W, Wang S, Wu D, Chen C, Luo Y, Pei Y, Tian B, Zhang J (2019) Fabrication of 3D Sponge@ $\text{AgBr-AgCl}/\text{Ag}$ and tubular photoreactor for continuous wastewater purification under sun-light irradiation. *ACS Sustain Chem Eng* 7:14051–14063. <https://doi.org/10.1021/acssuschemeng.9b02575>
- Kong W, Xing Z, Fang B, Cui Y, Li Z, Zhou W (2022) Plasmon Ag/Na-doped defective graphite carbon nitride/NiFe layered double hydroxides Z-scheme heterojunctions toward optimized photothermal-photocatalytic-Fenton performance. *Appl Catal B Environ* 304:120969. <https://doi.org/10.1016/j.apcatb.2021.120969>
- Kumar A, Sharma G, Naushad M, Muhtaseb AH, Penas AG, Mola GT, Si C, Stadler FJ (2020) Bio-inspired and biomaterials-based hybrid photocatalysts for environmental detoxification: a review. *Chem Eng J* 382:122937. <https://doi.org/10.1016/j.cej.2019.122937>
- Lakshmana Reddy N, Kumbhar VS, Lee K, Shankar MV (2020) Graphitic carbon nitride-based nanocomposite materials for photocatalytic hydrogen generation. *Nanostructured, Funct Flex Mater Energy Convers Storage Syst*. <https://doi.org/10.1016/B978-0-12-819552-9.00009-9>
- Lakshmana Reddy N, Navakoteswara Rao V, Mamatha Kumari M (2018) Nanostructured semiconducting materials for efficient hydrogen generation. Springer International Publishing
- Lee Y, Lee S, Kim HS, Moon JT, Joo JB, Choi I (2019) Multifunctional and recyclable TiO_2 hybrid sponges for efficient sorption, detection, and photocatalytic decomposition of organic pollutants. *J Ind Eng Chem* 73:328–335. <https://doi.org/10.1016/j.jiec.2019.02.001>
- Lee SY, Kang D, Jeong S, Do HT, Kim JH (2020) Photocatalytic degradation of rhodamine B dye by TiO_2 and Gold nanoparticles supported on a floating porous polydimethylsiloxane sponge under ultraviolet and visible light irradiation. *ACS Omega* 5:4233–4241. <https://doi.org/10.1021/acsomega.9b04127>
- Lee K, Sahu M, Hajra S, Abolhassani R, Mistewicz K, Toron B, Rubahn HG, Mishra YK, Kim HJ (2023) Zinc oxide tetrapod sponges for environmental pollutant monitoring and degradation. *J Mater Res Technol* 22:811–824. <https://doi.org/10.1016/j.jmrt.2022.11.142>
- Lei Z, Zhang G, Ouyang Y, Liang Y, Deng Y, Wang C (2017) Simple fabrication of multi-functional melamine sponges. *Mater Lett* 190:119–122. <https://doi.org/10.1016/j.matlet.2016.12.082>
- Li Z, Wang X, Xu N, Xiao Y, Ma L, Duan J (2020) Cost-effective and visible-light-driven melamine-derived sponge for tetracyclines degradation and Salmonella inactivation in water. *Chem Eng J* 394:124913. <https://doi.org/10.1016/j.cej.2020.124913>
- Li C, Kong W, Jin H (2022a) Construction of 3D sponge-like hierarchical pore $\text{Ag}_{10}\text{Si}_4\text{O}_{13}$ microblock photocatalyst with enhanced photocatalytic activities. *Colloids Surf A Physicochem Eng Asp* 633:127829. <https://doi.org/10.1016/j.colsurfa.2021.127829>
- Li Z, Bai H, Wei J, Kong L, Wang X, Xia X, Duan J (2022b) One-step synthesis of melamine-sponge functionalized carbon nitride for excellent water sterilization via photogenerated holes and photothermal conversion. *J Colloid Interface Sci* 610:893–904. <https://doi.org/10.1016/j.jcis.2021.11.126>

- Liang Q, Li Z, Yu X, Huang ZH, Kang F, Yang QH (2015) Macroscopic 3D porous graphitic carbon nitride monolith for enhanced photocatalytic hydrogen evolution. *Adv Mater* 27:4634–4639. <https://doi.org/10.1002/adma.201502057>
- Liang H, Guo J, Yu M, Zhan R, Liu C, Niu J (2021a) Porous loofah-sponge-like ternary heterojunction g-C₃N₄/Bi₂WO₆/MoS₂ for highly efficient photocatalytic degradation of sulfamethoxazole under visible-light irradiation. *Chemosphere* 279:130552. <https://doi.org/10.1016/j.chemosphere.2021.130552>
- Liang Q, Shao B, Tong S, Liu S, Tang L, Liu Y, Cheng M, He Q, Wu T, Pan Y, Huang J, Peng Z (2021b) Recent advances of melamine self-assembled graphitic carbon nitride-based materials: design, synthesis and application in energy and environment. *Chem Eng J* 405:126951. <https://doi.org/10.1016/J.CEJ.2020.126951>
- Lin D, Duan P, Yang W (2022a) Facile fabrication of melamine sponge@covalent organic framework composite for enhanced degradation of tetracycline under visible light. *Chem Eng J* 430:132817. <https://doi.org/10.1016/j.cej.2021.132817>
- Lin F, Gao M, Wang Y, Huang X, Zhao Y, Wang C, Pan Q (2022b) Enhanced mass transfer with amphiphilic CoOx/biochar for photocatalytic CO₂ conversion. *Appl Surf Sci* 605:154612. <https://doi.org/10.1016/j.apsusc.2022.154612>
- Liu Z, Cai X, Fan S, Zhang Y, Hu H, Huang Z, Liang J, Qin Y (2021) Preparation of a stable polyurethane sponge supported Sn-doped ZnO composite via double-template-regulated bionic mineralization for visible-light-driven photocatalytic degradation of tetracycline. *J Environ Chem Eng* 9:105541. <https://doi.org/10.1016/j.jece.2021.105541>
- Liu C, You J, Li Y, Zhu H, Xia L, Zhuang X (2023a) NaBiS₂ decorated polysaccharide sponges for adsorption–photocatalytic degradation of dye under visible light illumination. *Carbohydr Polym* 316:121072. <https://doi.org/10.1016/j.carbpol.2023.121072>
- Liu Y, Xia X, Gao Z, Ding J, Cheng X, Wei L (2023b) Stable photodegradation of antibiotics by the functionalized 3D-Bi₂MoO₆@MoO₃/PU composite sponge: high efficiency pathways, optical properties and Z-scheme heterojunction mechanism. *Chemosphere* 332:138911. <https://doi.org/10.1016/j.chemosphere.2023.138911>
- Ma X, Chai Y, Li P, Wang B (2019) Metal-organic framework films and their potential applications in environmental pollution control. *Acc Chem Res* 52:1461–1470. <https://doi.org/10.1021/acs.accounts.9b00113>
- Mi HY, Jing X, Napiwocki BN, Li NT, Turng LS, Huang HX (2018) Fabrication of fibrous silica sponges by self-assembly electrospinning and their application in tissue engineering for three-dimensional tissue regeneration. *Chem Eng J* 331:652–662. <https://doi.org/10.1016/J.CEJ.2017.09.020>
- Mudhoo A, Paliya S, Goswami P, Sing M, Lofrano G, Carotenuto, M, Carraturo F, Libralato G, Guida M, Usman M, Kumar S (2020) Fabrication, functionalization and performance of doped photocatalysts for dye degradation and mineralization: a review. Springer International Publishing
- Nagaraj S, Cheirmadurai K, Thanikaivelan P (2021) Visible-light active collagen-TiO₂ nanobio-sponge for water remediation: a sustainable approach. *Clean Mater* 1:100011. <https://doi.org/10.1016/j.clema.2021.100011>
- Paszkiwicz S, Szymczyk A (2019) Graphene-based nanomaterials and their polymer nanocomposites. *Nanomater Polym Nanocompos Raw Mater Appl*. <https://doi.org/10.1016/B978-0-12-814615-6.00006-0>
- Peçenek H, Dokan FK, Onses MS, Yilmaz E, Sahmetlioglu E (2022) Highly compressible binder-free sponge supercapacitor electrode based on flower-like NiO/MnO₂/CNT. *J Alloys Compd* 913:165053. <https://doi.org/10.1016/J.JALLCOM.2022.165053>
- Peng Z, Tang H, Yao K (2015) Recyclable TiO₂/carbon nanotube sponge nanocomposites: controllable synthesis, characterization and enhanced visible light photocatalytic property. *Ceram Int* 41:363–368. <https://doi.org/10.1016/j.ceramint.2014.08.079>
- Peng M, Zhu Y, Li H, He K, Zeng G, Chen A, Huang Z, Huang T, Yuan L, Chen G (2019) Synthesis and application of modified commercial sponges for oil-water separation. *Chem Eng J* 373:213–226. <https://doi.org/10.1016/j.cej.2019.05.013>
- Picó Y, Alvarez-Ruiz R, Alfarhan AH, El-Sheikh MA, Alshahrani HO, Barcelo D (2020) Pharmaceuticals, pesticides, personal care products and microplastics contamination assessment of Al-Hassa irrigation network (Saudi Arabia) and its shallow lakes. *Sci Total Environ* 701:135021. <https://doi.org/10.1016/j.scitotenv.2019.135021>
- Qu Y, Xu X, Huang R, Qi W, Su R, He Z (2020) Enhanced photocatalytic degradation of antibiotics in water over functionalized N, S-doped carbon quantum dots embedded ZnO nanoflowers under sunlight irradiation. *Chem Eng J* 382:123016. <https://doi.org/10.1016/J.CEJ.2019.123016>
- Rajagopal S, Paramasivam B, Muniyasamy K (2020) Photocatalytic removal of cationic and anionic dyes in the textile wastewater by H₂O₂ assisted TiO₂ and micro-cellulose composites. *Sep Purif Technol* 252:117444. <https://doi.org/10.1016/j.seppur.2020.117444>
- Rostamabadi H, Falsafi SR, Boostani S, Katouzian I, Rezaei A, Assadpour E, Jafari SM (2021) Design and formulation of nano/micro-encapsulated natural bioactive compounds for food applications. *Appl Nano/microencapsulated Ingredients Food Prod*. <https://doi.org/10.1016/B978-0-12-815726-8.00001-5>
- Sahoo SK, Manoharan B, Sivakumar N (2018) Introduction: Why perovskite and perovskite solar cells? Perovskite photovoltaics basic to adv concepts implement. <https://doi.org/10.1016/B978-0-12-812915-9.00001-0>
- Sam EK, Liu J, Lv X (2021) Surface engineering materials of superhydrophobic sponges for oil/water separation: a review. *Ind Eng Chem Res* 60:2353–2364. <https://doi.org/10.1021/acs.iecr.0c05906>
- Sarkar S, Ponce NT, Banerjee A, Bandopadhyay R, Rajendran S, Lichfouse E (2020) Green polymeric nanomaterials for the photocatalytic degradation of dyes: a review. *Environ Chem Lett* 18:1569–1580. <https://doi.org/10.1007/s10311-020-01021-w>
- Scaria J, Nidheesh AKV, PV (2021) Tetracyclines in the environment: an overview on the occurrence, fate, toxicity, detection, removal methods, and sludge management. *Sci Total Environ* 771:145291. <https://doi.org/10.1016/J.SCITOTENV.2021.145291>
- She P, Xu K, Yin S, He Q, Zeng S, Sun H, Liu Z (2018) Bioinspired self-standing macroporous Au/ZnO sponges for enhanced photocatalysis. *J Colloid Interface Sci* 514:40–48. <https://doi.org/10.1016/j.jcis.2017.12.003>
- Shi H, Ni J, Zheng T, Wang X, Wu C, Wang Q (2020) Remediation of wastewater contaminated by antibiotics. *Rev Environ Chem Lett* 18:345–360. <https://doi.org/10.1007/s10311-019-00945-2>
- Sirajudheen P, Poovathumkuzhi NC, Vigneshwaran S, Chelaveetil BM, Meenakshi S (2021) Applications of chitin and chitosan based biomaterials for the adsorptive removal of textile dyes from water—a comprehensive review. *Carbohydr Polym* 273:118604. <https://doi.org/10.1016/J.CARBPOL.2021.118604>
- Sosnin IM, Vlassov S, Dorogin LM (2021) Application of polydimethylsiloxane in photocatalyst composite materials: a review. *React Funct Polym* 158:104781. <https://doi.org/10.1016/j.reactfunctpolym.2020.104781>
- Su Y, Li S, He D, Yu D, Liu F, Shao N, Zhang Z (2018) MOF-derived porous ZnO nanocages/rGO/carbon sponge-based photocatalytic microreactor for efficient degradation of water pollutants and hydrogen evolution. *ACS Sustain Chem Eng* 6:11989–11998. <https://doi.org/10.1021/acssuschemeng.8b02287>

- Sui S, Quan H, Hu Y, Hou M, Guo S (2021) A strategy of heterogeneous polyurethane-based sponge for water purification: combination of superhydrophobicity and photocatalysis to conduct oil/water separation and dyes degradation. *J Colloid Interface Sci* 589:275–285. <https://doi.org/10.1016/j.jcis.2020.12.122>
- Sukul M, Sahariah P, Lauzon HL, Borges J, Masson M, Mano JF, Haugen HJ, Reseland JE (2021) In vitro biological response of human osteoblasts in 3D chitosan sponges with controlled degree of deacetylation and molecular weight. *Carbohydr Polym*. <https://doi.org/10.1016/j.carbpol.2020.117434>
- Sun S, Tang Q, Yu T, Gao Y, Zhang W, Zhou L, Elhegazy H, He K (2022) Fabrication of g-C₃N₄@Bi₂MoO₆@AgI floating sponge for photocatalytic inactivation of microcystis aeruginosa under visible light. *Environ Res* 215:114216. <https://doi.org/10.1016/J.ENVRES.2022.114216>
- Tahir T, Chaudhary K, Warsi MF, Saif MS, Alsafari IA, Shakir I, Agbool PO, Haider S, Zulfigar S (2022) Synthesis of sponge like Gd³⁺ doped vanadium oxide/2D MXene composites for improved degradation of industrial effluents and pathogens. *Ceram Int* 48:1969–1980. <https://doi.org/10.1016/j.ceramint.2021.09.282>
- ten Elshof JE (2015) Chemical solution deposition techniques for epitaxial growth of complex oxides. *Ep Growth Complex Met Oxides*. <https://doi.org/10.1016/B978-1-78242-245-7.00004-X>
- Tijani JO, Fatoba OO, Babajide OO, Petrik LF (2016) Pharmaceuticals, endocrine disruptors, personal care products, nanomaterials and perfluorinated pollutants: a review. *Environ Chem Lett* 14:27–49. <https://doi.org/10.1007/s10311-015-0537-z>
- Timusk M, Nigol IA, Vlassov S, Oras S, Kangur T, Linarrts A, Sutka A (2022) Low-density PDMS foams by controlled destabilization of thixotropic emulsions. *J Colloid Interface Sci* 626:265–275. <https://doi.org/10.1016/j.jcis.2022.06.150>
- Tu C, Dong ZR, Yan C, Guo Y, Cui L (2019) A pH indicating carboxymethyl cellulose/chitosan sponge for visual monitoring of wound healing. *Cellulose* 26:4541–4552. <https://doi.org/10.1007/s10570-019-02378-0>
- Tu X, Ke S, Luo S, Zhou R, Zeng Z, Luo S (2021) Self-supporting rGO/BiOBr composite on loofah-sponge as a floating monolithic photocatalyst for efficient microcystis aeruginosa inactivation. *Sep Purif Technol* 275:119226. <https://doi.org/10.1016/j.seppur.2021.119226>
- Usman M, Zeb Z, Ullah H, Suliman MH, Humayun M, Ullah L, Shah SNA, Ahmed U, Saeed M (2022) A review of metal-organic frameworks/graphitic carbon nitride composites for solar-driven green H₂ production, CO₂ reduction, and water purification. *J Environ Chem Eng* 10:107548. <https://doi.org/10.1016/j.jece.2022.107548>
- Wang F, Zhou Y, Li P, Li H, Tu W, Yan S, Zou Z (2014) Formation of 3D interconnectively macro/mesoporous TiO₂ sponges through gelation of lotus root starch toward CO₂ photoreduction into hydrocarbon fuels. *RSC Adv* 4:43172–43177. <https://doi.org/10.1039/c4ra06565d>
- Wang H, Wang G, Liu Z, Jin Z (2018a) Strategy of nitrogen defects sponge from g-C₃N₄ nanosheets and Ni-Bi-Se complex modification for efficient dye-sensitized photocatalytic H₂ evolution. *Mol Catal* 453:1–11. <https://doi.org/10.1016/j.mcat.2018.04.028>
- Wang W, An T, Li G, Li Y, Yu JC, Wong PK (2018b) Free-standing red phosphorus/silver sponge monolith as an efficient and easily recyclable macroscale photocatalyst for organic pollutant degradation under visible light irradiation. *J Colloid Interface Sci* 518:130–139. <https://doi.org/10.1016/j.jcis.2018.02.008>
- Wang Y, Zhao S, Zhang Y, Chen W, Yuan S, Zhou Y, Huang Z (2019) Synthesis of graphitic carbon nitride with large specific surface area via copolymerizing with nucleobases for photocatalytic hydrogen generation. *Appl Surf Sci* 463:1–8. <https://doi.org/10.1016/J.APSUSC.2018.08.215>
- Wang S, Yan F, Ren P, Li Y, Wu Q, Fang X, Chen F, Wang C (2020a) Incorporation of metal-organic frameworks into electrospun chitosan/poly (vinyl alcohol) nanofibrous membrane with enhanced antibacterial activity for wound dressing application. *Int J Biol Macromol* 158:9–17. <https://doi.org/10.1016/J.IJBIOMAC.2020.04.116>
- Wang Y, Wang K, Lin J, Wang X (2020b) The preparation of nano-MIL-101(Fe)/chitosan hybrid sponge and its rapid and efficient adsorption to anionic dyes. *Int J Biol Macromol* 165:2684–2692. <https://doi.org/10.1016/J.IJBIOMAC.2020.10.073>
- Wang W, Zhou C, Yang Y, Zeng G, Zhang C, Zhou Y, Yang J, Huang D, Wang H, Xiong W, Li X, Fu Y, Wang Z, He Q, Jia M, Luo H (2021) Carbon nitride based photocatalysts for solar photocatalytic disinfection, can we go further? *Chem Eng J* 404:126540. <https://doi.org/10.1016/j.cej.2020.126540>
- Wang M, Zhang Y, Chen D, Li N, Xu Q, Li H, Lu J (2023) Biomimetic porphyrin-modified 3D porous composite material adsorption enhances photocatalytic CO₂ reduction and tetracycline oxidative degradation. *Chem Eng J* 469:144064. <https://doi.org/10.1016/j.cej.2023.144064>
- Wen J, Xie J, Chen X, Li X (2017) A review on g-C₃N₄-based photocatalysts. *Appl Surf Sci* 391:72–123. <https://doi.org/10.1016/J.APSUSC.2016.07.030>
- Xu P, Yang J, Chen Y, Li Y, Jia X, Song H (2019) Wood-derived fiber/BiOBr/AgBr sponges by in situ synthesis for separation of emulsions and degradation of dyes. *Mater Des* 183:108179. <https://doi.org/10.1016/J.MATDES.2019.108179>
- Xu X, Yu J, Liu C, Yang G, Shi L, Zhuang X (2021) Xanthated chitosan/cellulose sponges for the efficient removal of anionic and cationic dyes. *React Funct Polym* 160:104840. <https://doi.org/10.1016/j.reactfunctpolym.2021.104840>
- Yang Y, Zhang Q, Zhang R, Ran T, Wan W, Zhou Y (2018) Compressible and recyclable monolithic g-C₃N₄/melamine sponge: a facile ultrasonic-coating approach and enhanced visible-light photocatalytic activity. *Front Chem* 6:1–10. <https://doi.org/10.3389/fchem.2018.00156>
- Yang B, Zheng Y, Wen Y, Zhang T, Lin M, Yan J, Zhuang Z, Yu Y (2022) Sponge-like nickel carbonate of high porosity and carbonate vacancy for high-performance CO₂ photoreduction. *Adv Sustain Syst*. <https://doi.org/10.1002/advs.202100494>
- Yao F, Dai L, Bi J, Xue W, Deng J, Fang C, Zhang L, Zhao H, Zhang W, Xiong P, Fu Y, Sun J, Zhu J (2022) Loofah-like carbon nitride sponge towards the highly-efficient photocatalytic transfer hydrogenation of nitrophenols with water as the hydrogen source. *Chem Eng J* 444:136430. <https://doi.org/10.1016/j.cej.2022.136430>
- You J, Liu C, Feng X, Lu B, Xia L, Zhuang X (2022) In situ synthesis of ZnS nanoparticles onto cellulose/chitosan sponge for adsorption-photocatalytic removal of Congo red. *Carbohydr Polym* 288:119332. <https://doi.org/10.1016/J.CARBPOL.2022.119332>
- Yu P, Zhou X, Yan Y, Li Z, Zheng T (2019) Enhanced visible-light-driven photocatalytic disinfection using AgBr-modified g-C₃N₄ composite and its mechanism. *Colloids Surf B Biointerfaces* 179:170–179. <https://doi.org/10.1016/j.colsurfb.2019.03.074>
- Zhan X, Zhao Y, Sun Y, Wang H (2022) Pyridazine doped g-C₃N₄ with nitrogen defects and spongy structure for efficient tetracycline photodegradation and photocatalytic H₂ evolution. *Chemosphere* 307:136087. <https://doi.org/10.1016/J.CHEMOSPHERE.2022.136087>
- Zhang F, Zhang S, Zou S, Zhong S (2016a) Facile synthesis of sponge-loaded Bi₂WO₆ photocatalyst and degradation of tetracycline hydrochloride under visible light. *J Mater Sci Mater Electron* 27:12141–12147. <https://doi.org/10.1007/s10854-016-5367-7>
- Zhang W, Li Y, Peng S (2016b) Facile synthesis of graphene sponge from graphene oxide for efficient dye-sensitized H₂ evolution.

- ACS Appl Mater Interfaces 8:15187–15195. <https://doi.org/10.1021/acsami.6b01805>
- Zhang F, Song N, Zhang S (2017a) Synthesis of sponge-loaded $\text{Bi}_2\text{WO}_6/\text{ZnFe}_2\text{O}_4$ magnetic photocatalyst and application in continuous flow photocatalytic reactor. *J Mater Sci Mater Electron* 28:8197–8205. <https://doi.org/10.1007/s10854-017-6530-5>
- Zhang T, Liang W, Huang Y, Li X, Liu Y, Yang B, He C, Zhou X, Zhang J (2017b) Bifunctional organic sponge photocatalyst for efficient cross-dehydrogenative coupling of tertiary amines to ketones. *Chem Commun* 53:12536–12539. <https://doi.org/10.1039/c7cc06997a>
- Zhang R, Ma M, Zhang Q (2018) Multifunctional g-C₃N₄/graphene oxide wrapped sponge monoliths as highly efficient adsorbent and photocatalyst. *Appl Catal B Environ* 235:17–25. <https://doi.org/10.1016/j.apcatb.2018.04.061>
- Zhang D, Wang L, Zeng H, Yan P, Nie J, Sharma VK, Wang C (2019a) A three-dimensional macroporous network structured chitosan/cellulose biocomposite sponge for rapid and selective removal of mercury(II) ions from aqueous solution. *Chem Eng J* 363:192–202. <https://doi.org/10.1016/j.cej.2019.01.127>
- Zhang T, Sanguramath RA, Israel S, Silverstein MS (2019b) Emulsion templating: porous polymers and beyond. *Macromolecules* 52:5445–5479. <https://doi.org/10.1021/acs.macromol.8b02576>
- Zhang Y, Yin X, Yu B, Wang X, Guo Q, Yng J (2019c) Recyclable polydopamine-functionalized sponge for high-efficiency clean water generation with dual-purpose solar evaporation and contaminant adsorption. *ACS Appl Mater Interfaces* 11:32559–32568. <https://doi.org/10.1021/acsami.9b10076>
- Zhang T, Chang F, Qi Y, Zhang X, Yang J, Liu X, Li S (2020) A facile one-pot and alkali-free synthetic procedure for binary $\text{SnO}_2/\text{g-C}_3\text{N}_4$ composites with enhanced photocatalytic behavior. *Mater Sci Semicond Process* 115:105112. <https://doi.org/10.1016/j.mssp.2020.105112>
- Zhang H, Li L, Geng L, Tan X, Hu Y, Mu P (2023) Reduced graphene oxide/carbon nitride composite sponge for interfacial solar water evaporation and wastewater treatment. *Chemosphere* 311:137163. <https://doi.org/10.1016/j.chemosphere.2022.137163>
- Zhao X, Wang X, Lou T (2022) Simultaneous adsorption for cationic and anionic dyes using chitosan/electrospun sodium alginate nanofiber composite sponges. *Carbohydr Polym* 276:118728. <https://doi.org/10.1016/j.carbpol.2021.118728>
- Zhao T, Cheng H, Liang Y (2020) Preparation of TiO_2 /sponge composite for photocatalytic degradation of 2,4,6-trichlorophenol, water, air & soil. <https://doi.org/10.1007/s11270-020-04774-w>
- Zhou P, Qin B, Zhang L, Wu Z, Dai Y, Hu C, Xu H, Mao Z (2023) Facile construction of photocatalytic cellulose-based sponge with stable flotation properties as efficient and recyclable photocatalysts for sewage treatment. *Int J Biol Macromol* 239:124233. <https://doi.org/10.1016/j.ijbiomac.2023.124233>
- Zhu D, Handschuh-Wang S, Zhou X (2017) Recent progress in fabrication and application of polydimethylsiloxane sponges. *J Mater Chem A* 5:16467–16497

Publisher's Note Springer Nature remains neutral with regard to jurisdictional claims in published maps and institutional affiliations.

Springer Nature or its licensor (e.g. a society or other partner) holds exclusive rights to this article under a publishing agreement with the author(s) or other rightsholder(s); author self-archiving of the accepted manuscript version of this article is solely governed by the terms of such publishing agreement and applicable law.